Universitat Autònoma
de Barcelona

Master's Thesis

Master in Telecommunication Engineering

Electronic Design for a fully wireless smart insole

Borja Herranz Pérez

Supervisor: Jordi Carrabina Bordoll & Marc Codina Barbera

Departament de Microelectrònica i Sistemes Electrònics

Escola d'Enginyeria (EE)

Universitat Autònoma de Barcelona (UAB)

UAB

Els sotasignants, *Jordi Carrabina Bordoll i Marc Codina Barbera*, Professors de l'Escola d'Enginyeria (EE) de la Universitat Autònoma de Barcelona (UAB),

CERTIFIQUEN:

Que el projecte presentat en aquesta memòria de Treball Final de Master ha estat realitzat sota la seva direcció per l'alumne *Borja Herranz Pérez*

I, perquè consti a tots els efectes, signa el present certificat.

Bellaterra, *4 de Setembre de 2019*

Signatura: *Jordi Carrabina Bordoll* *Marc Codina Barbera*

Resum:

Aquesta tesi representa el disseny d'una plantilla dissenyada per detectar caigudes i monitoritzar i caracteritzar els passos al caminar amb l'objectiu de minimitzar el risc de caigudes, especialment en gent gran. La plantilla és prou prima com per ser confortable per a l'usuari i no te cap contacte elèctric. El prototip incorpora tecnologies avançades com Bluetooth 5, plaques de circuit imprès flexi-rígides, sensors MEMS i tèxtils, càrrega per inducció i interruptors magnètics. Aquestes característiques permeten que la plantilla funcioni en una àmplia varietat d'entorns sense el risc d'un mal funcionament a causa de la humitat o la suor.

Resumen:

Esta tesis presenta el diseño de una plantilla diseñada para detectar caídas y en 1monitorizar y caracterizar los pasos al caminar con objeto de minimizar el riesgo de caídas, especialmente en gente mayor. La plantilla es lo suficientemente delgada para ser confortable para el usuario y no tiene ningún contacto eléctrico. El prototipo incorpora tecnologías avanzadas como Bluetooth 5, placas de circuito impreso flexi-rígidas, sensores MEMS e textiles, carga por inducción e interruptores magnéticos. Estas características permiten que la plantilla funcione en una amplia variedad de entornos sin riesgo de un mal funcionamiento debido a la humedad o al sudor.

Summary:

This thesis presents the design of a fully wireless insole for detecting falls and monitoring and characterizing gait with the goal of reducing fall risk specially for the elderly. The insole is thin enough to be comfortable for the user. The prototype incorporate advanced technologies like Bluetooth 5, rigid-flex PCB, MEMS and textile sensors, induction charging and magnetic switches. These features allow the insole to operate in a wide variety of environments without the risk of malfunction due to humidity or sweat.

Index

Figures

Introduction

IoT devices are becoming more and more popular among different communities, which has caused manufacturers from all other the world to present new affordable and innovative solutions into the market.

Among these devices, health-care non-invasive devices are experiencing a huge success. The best examples are the activity trackers like FitBit or sport oriented smart-watches. But other ideas are being explored, opening the market. To name a few Smart continuous glucose monitoring and insulin pens[1], Bluetooth-enabled coagulation system[2] and Asthma Monitor[3].

This expansion in the market allow the opportunity to develop other devices, in-tune with the demand of the consumer of way to monitor their day to day to achieve a healthier life.

This thesis represent the first iteration of the design of a fully wireless insole for detecting falls, monitoring gait and activity tracker.

Objectives

The main objectives of this project is the design of a fully wireless insole for detecting falls, monitoring gait and activity tracker.

Some of the specifications that the insole must accomplish are:

The insole should thin enough to go unnoticed for the user and thus not creating a bias in their steps. With aim to improve the diagnosis, treatment and ultimately alert in case of falling of people wearing the insoles independently of the environment thus with the requisite to work either in indoor or outdoor areas.

The insole must operate in a wide variety of environments without the risk of malfunction due to humidity or sweat. Allowing the use in high intensity activities (aka sport exercises) and somewhat resilience against weather and daily life incidents.

Scope of the project

To achieve the objectives of this project, a prototype incorporating advanced technologies like Bluetooth SoCs, rigid-flex PCB, u-Vias, piezoelectric textiles and MEMS sensors, induction charging, magnetic switches, full spatial position sensor and LPWAN technologies.

Also a basic test plant will be developed to check if the individual functionality as BLE, spatial positioning, ADC conversion and LoRa communications are working hence creating a blank canvas to produce firmware.

Architecture & Hardware

Architecture

First step in designing any embedded system is creating a list with the requirements needed to develop the insole electronics. This will allow creating a high-level abstraction schematic. Figure 1 shows the proposed architecture that takes into account the requirements.

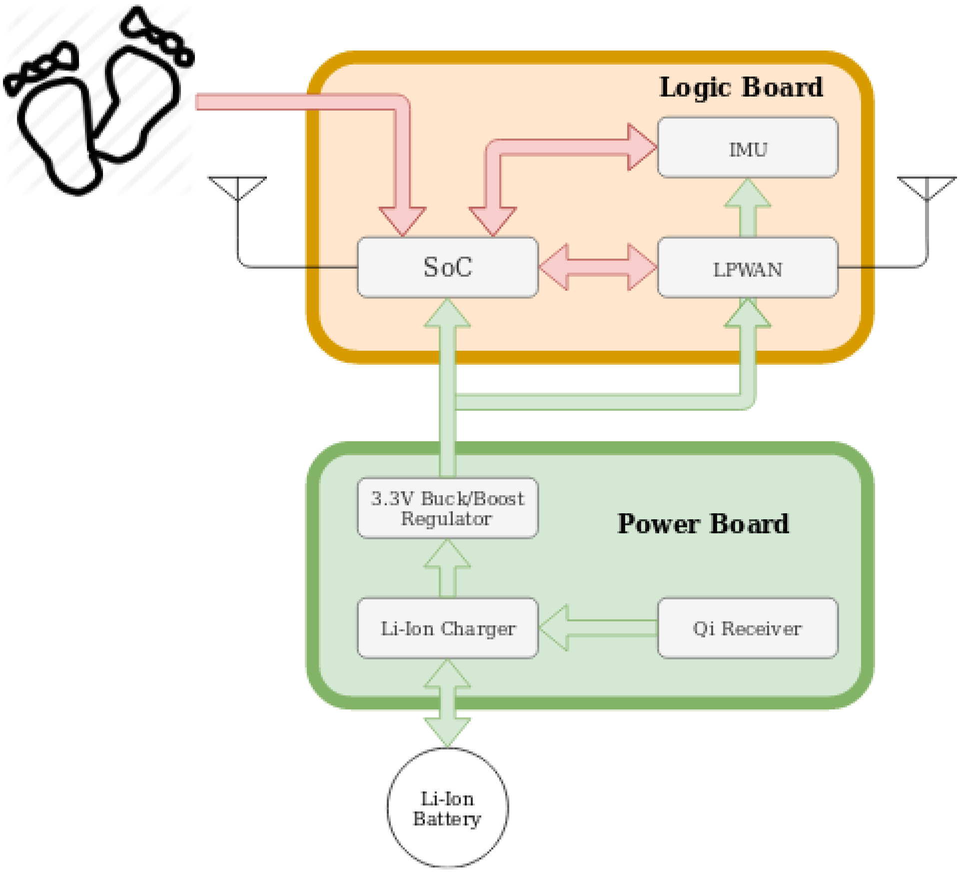

Figure 1 Architecture of the system

The hardware will be divided into two mayor sub-assemblies called logic or functional board and power board. Intuitively, the logic board will allow communication between the electronic components of a system, such as the micro-controller (MCU) and sensors (pressure, IMU) and provides connectors for other peripherals.

Additionally to the MCU, the logic board has others peripherals that allow recording data so that the information could be the most accurate possible.

Thanks to the smartphone market booming in the past years, minituarization of components, specially sensors, is astonishing. For that reason, it is possible to incorporate a 9 axis inertial measurement unit (IMU) in the insole design.

A 9-Axis is preferable because the margin in terms of size and cost compared to other IMU with inferior number of axes is negligible and the magnetometer could provide a useful heading reference.

Since the amount of data generated by the insole sensors will be quite significant and in the proposed architecture there is no data storage system as a saving measure in terms of power and area, the Bluetooth Low Energy radio link (onward BLE) in the SoC is vital for the design.

This will allow transmitting all data from both insoles to a BLE connected device, usually a smartphone. At the same time, in the case than the insole will be used as a fall detection alert system, a long-range low-power radio has been selected. This one does not require high bandwidth (as from BLE). This will give an all-around coverage in communications.

Similarly, the power board will hold all the components that allow managing wireless charging, storage in a lithium chemistry battery, due to the high density energy that they provide, and generate a stable power rail for the logic board through a DC-DC converter.

The fact that both boards will be physically separated will provide higher electromagnetic compatibility advantage isolating power inductor from the DC-DC converter and the wireless power transmitter and the LPWAN antennas.

Besides all the previous discussed, the hardware must be as small as possible. Areas where electronics can survive the stress of the forces created in the insole are very limited. Areas with low pressure (from the weight of the human body) are of interest to increase reliability and to minimize the bias on the gait pattern.
As shown in figure 2, a pressure map of the foot extracted from *Plantar pressure distribution and gait stability: Normal VS high heel*[4]

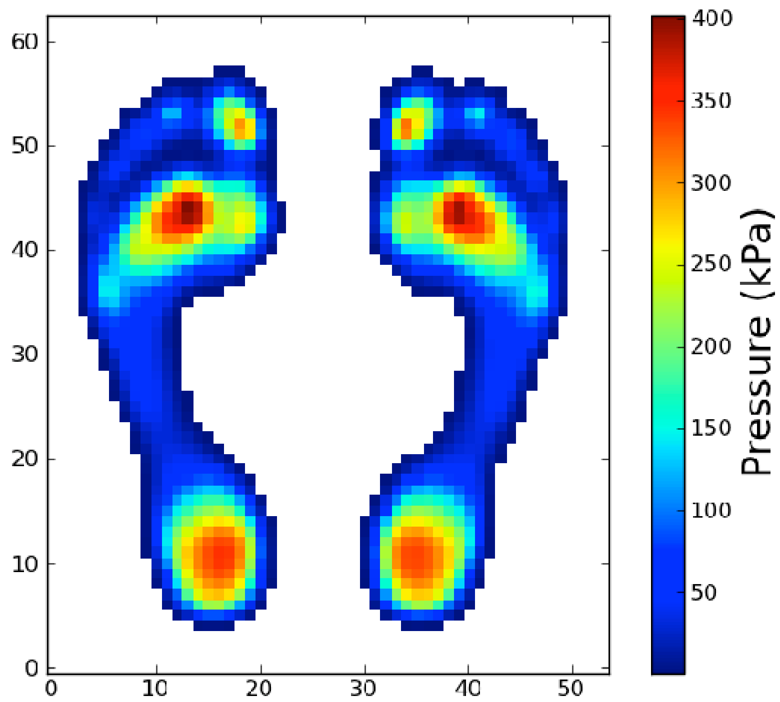

Figure 2 Foot pressure map

The best usable zones o place the electronics is the instep arch, where the pressure is minimum, around 50kPa.

Hardware

Once the system architecture is fixed, you have to look for electronic components that meet the requirements. Websites like Octopart[5] , a searcher for the different manufacturers and distributors is a good place to start.

Also generic web-searchers like Google or DuckDuckgo are good places to start and because they use different search engines, same query will bring different results.

Logic Board

MCU SoC

For the main MCU SoC, the component selected is the STM32WB55. The main reason to use this specific microcontroller is because is a SoC (system on chip) which means that within the silicon die, there are multiple HW cores working as one system. In our case, this IC provides a classic micro-controller with GPIO, ADC, Timers, etc. while also integrating a BLE 5 modem.

There are other SoCs that provide similar characteristics like the NRF52 from Nordic Semiconductors. The ST SoC has been selected because I have previous experience with the STM32 family, the support for the LoRaWAN stack and the low consumption in sleep mode, one of the best of the market. Its main features are shown in the picture 3.

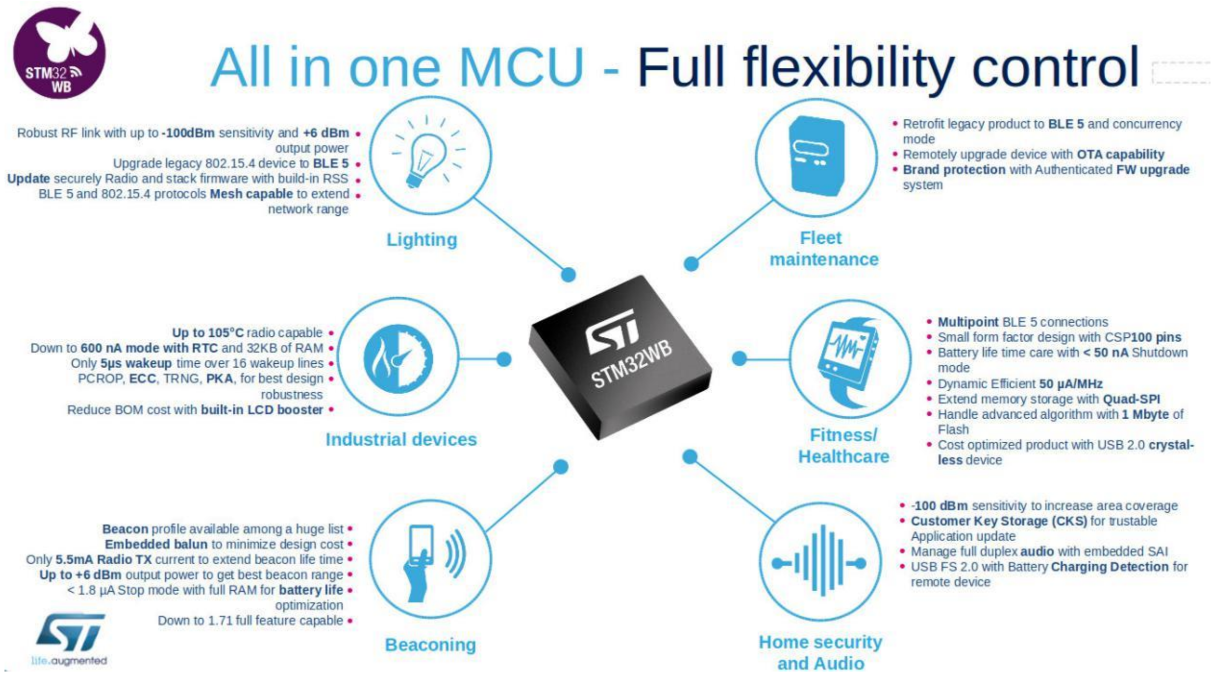

Figure 3 Main feature of the STM32WB

The SW development for this MCU is done thanks to the STM CUBEMX tool and the HAL libraries. This framework is a set of libraries and tools needed for the whole STM32 MCU family.

STM32 CubeMX and the toolchain to build and flash the app into the STM32 can be installed on Windows, Linux and MacOS operating systems[6]. After experimenting with both Windows and Linux installations, because of third-party IDE support is better for Windows systems the choice to develop in windows is a no-brainer.

Pressure Sensor

For the pressure sensors the most interesting option is the use of a custom solution offered by a Barcelona-area company called Sensingtex[7].

This company specializes in smart textiles, capable of create pressure sensors flexible enough to bond with a piece of cloth and don't affect the flexibility or tactile feeling.

Their sensors are build using a conductive, non-woven microfiber with piezo-resistive functionality that allow for use in dynamic sensors to map and measure pressure, bend, angle stretch and torsion and depending on the layers compositions. Sensors can read pressures up to 700 psi. Combined with their ability to print conductive traces using silkscreen technology with a resulting thickness around 200μm makes perfect sense to develop a solution using their technology.

The custom sensor has 6 pressure points positioned all over the foot footprint in strategical selected points to allow to read the dynamic movements of the person with high resolution.

Figure 4 shows the layering composed with the piezo-resistive material and the substrate for the conductive traces.

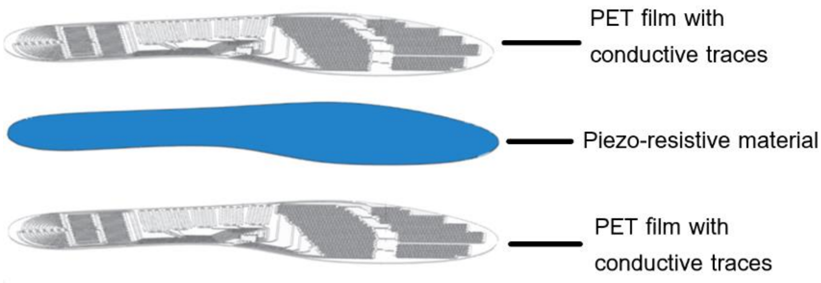

Figure 4 Layering of the pressure sensor

IMU

This compact module includes tri-axis accelerometer, gyroscope and magnetometer that measure the acceleration, angular speed and magnetic forces on the component. These three elements form an orthogonal reference system.

Adding to the definition stated before, the BNO055 enhance all the information of a "traditional" IMU being a System in Package (SiP) running on-board Sensor Fusion[8] and integrating :

- Triaxial 14-bit accelerometer.
- Triaxial 16-bit gyroscope with a range of ±2000 degrees per second.
- Triaxial geomagnetic sensor.
- And a 32-bit microcontroller running the company's BSX3.0 FusionLib software.

Adding an MCU allows performing calculations such that this system can provide both the position and orientation of the object referred to the system, at just 5.2 x 3.8 x 1.1 mm^3, what is significantly smaller than comparable discrete or system-on-board solutions.

LPWAN

From all the hardware here explain, the LPWAN modem maybe the most unknown among the public because of its recent development.

LPWAN are wireless technology oriented to the Internet of Things segment, allowing longer ranges at lower energy consumption rates, by using sub-GHz bands. The most prominent LPWAN technologies are Sigfox, NB-IoT and LoRa.

Sigfox

Sigfox is the most widespread worldwide LPWAN communication network for IoT, covering nearly 98% of the European and American territory. The Sigfox network is built on an ultra-narrow band modulation and operates in the 868MHz band in Europe and 920MHz in the United States.

One of the main reasons for the use of Sigfox today, apart from having an almost global deployment and coverage, is that the manufacturers of IoT devices have adapted to their technology and facilitate the uploading of data to the cloud of this network being available on the company's servers for access through any Internet connection. To this must be added the support available from Microsoft's Azure, a cloud service hosted in Microsoft's Data Centers. This greatly accelerates the execution of an IoT project.

The low cost of this technology, its acceptance by device manufacturers, or whether it is a bidirectional network are other factors in favor. On the contrary, as it is an unlicensed frequency, that is, a band of frequencies in which the operation of radio-communication devices is allowed without a centralized planning on the part of the Communications Authority, without an individual authorization of each station such as to ensure the assignment of a frequency or channel for exclusive use of the same, it could be in the future out of the market, since this frequency could be regulated by the public organisms and acquired by the sector of the large telecommunications companies, which want to bet on M2M or NB IoT[9].

NB-IoT

Evolution of LTE/4G adapted to IoT (Cat M1 or Cat M and Cat NB or NB-IoT mainly). This other network with LPWAN technology is the great bet of the telecommunication operators at global level. It is the network for which Vodafone has always bet and has taken an important step for its development completing successfully the first roaming connection in Europe. It has its differential factor in that its operating spectrum falls within the range of the LTE or 4G, so that its deployment and commercial exploitation is almost assured thanks to the network currently deployed. It has a higher bandwidth and consumption than LoRa and Sigfox. In Spain, the strongest bet so far is Vodafone, which in 2017 announced the commercial deployment of NB IoT.

The main disadvantage of NB IoT was the roaming between networks of different operators, but that stumbling block is the one that has just been overcome with the first NB IoT connection in Europe between the networks Vodafone in Spain and Deutsche Telekom in Austria. With global SIM cards, NB IoT modules from each operator have been able to complete connections in each other's network without major problems

LoRa

LoRa is another LPWAN network with a business model very similar to Sigfox, although with a somewhat different technology. Among other aspects, it uses a communication spectrum wider than SigFox. If you are looking for a considerable difference between the two networks, LoRa is an LPWAN network better prepared for bidirectional communication in real time with the IoT device. Also, the specifications for manufacturers who want to communicate their equipment through LoRa are more open or less than strict than with Sigfox. On the other hand, LoRa's coverage is much less than Sigfox's, as it is currently only deployed in France, Belgium, Switzerland, the Netherlands and South Africa, which is undoubtedly a determining factor when planning an IoT project.

The modulation technology used is called CSS and is radio-frequency like AM or FM. It has been used in military and space communications for decades. Its great advantage is that it can communicate over long distances and is very resistant to interference.[10]

LoRa significantly improves receiver sensitivity and, as with other spread spectrum modulation techniques, uses the channel bandwidth to transmit a signal, making it robust to channel noise and insensitive to frequency compensation. It can demodulate 19.5dB signals below the noise level; while most FSK frequency offset systems require 8-10dB signal power above the noise level to demodulate properly.

This low-power, long-range wireless connectivity network maintains a data rate of 0.3 kbps to 50 kbps depending on the range and duration of the message. Transmission distances can be up to 15 or 20 km in rural environments.

The maximum size of user data depends on the speed of the data. For minimum and maximum data rates in Europe, the maximum data sizes are respectively 59 and 250 bytes. As the preamble of LoRa, a set of ones and zeros that precede the incoming data, is composed of eight symbols, a node can spend a lot of time in Rx mode, Tx response, depending on the chosen. However, precise synchronization of the nodes is required to achieve the LoRa coding gain needed to demodulate the LoRa signal below the noise threshold.

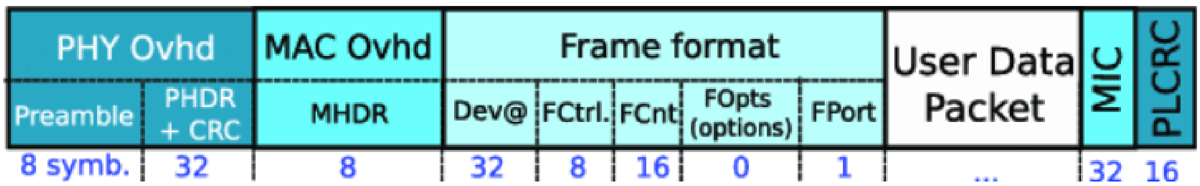

Figure 5 LoRa data packet structure

LoRa technology was originally developed by Semetech, but is currently managed by LoRa Alliance. Thus, any hardware manufacturer wishing to work with this technology must be certified by the alliance.

This connectivity system responds to the specifications required by the prototype in which it is working as bidirectional, mobility or geo-localization. Among other things the LoRa network is interesting for:

- ❖ High tolerance to interference.
- ❖ High sensitivity to receive data (-168dB).
- ❖ Based on chirp modulation.
- ❖ Low power consumption (up to 10 years with a battery).
- ❖ Long range (up to 15km in rural environments).
- ❖ Low data transfer (up to 250bytes).
- ❖ Point-to-point connection.
- ❖ Working frequencies of 868MHz in Europe, 915MHz in America and 433MHz in Asia.

All this makes it an ideal technology for long-distance connections and for IoT networks where sensors are needed that do not have large energy consumption. For them, it has great application possibilities for Smart Cities, places with little cellular coverage such as agricultural or livestock applications in the field, or to build private networks of sensors. With all this information, the logic assumption is to use a LoRa connection in the LPWAN modem of the architecture.

Combining the **Bluetooth** 5 integrated in the SoC STM32WB55 and this LoRa modem, the requisite to have a complete coverage no matter if the insole is inside or outside buildings is achieved. Granted that 100% it's never possible but the situations when the system won't work due to interference will be far and few between.

Power Board

For the power board design, we need to make a rough estimation of the energy consumption of the system since two important factors depend on it: the maximum current to supply from the DC/DC converter and the battery capacity which at the end is the key factor to a longer active period.
For this energy consumption estimation, the worst-case scenario is assuming

that all devices are active and at peak consumption.

Device	mA
STM32WB55	11.7
BNO055	12.3
SX1276	120
Total	~150

Figure 6. Energy Consumption Estimation

DC/DC converter

With this estimation, we can see that a DC/DC converter capable of more than 150mA is needed. Also, this DC/DC converter will have to be capable of reducing the input voltage from the battery to provide 3.3v for the circuits. These are usually known as buck/boost converters.

This requirement will become obvious in the later point "Batteries" where due to the chemistry of the battery and to elongate the battery life this will become a relevant characteristic.

For this purpose, the TPS6303X is the most obvious choice. It is a converter which is already experienced in IoT devices, with the input range from 1.8v to 5.5v and capable to provide 800mA @ 3.3v in Step-Down mode and 500mA @ 3.3v in Step-Up Mode.

Other features are:

- Up to 96% Efficiency
- Automatic Transition Between Step-Down and Boost Mode
- Device Quiescent Current less than 50 μA
- Power-Save Mode for Improved Efficiency at Low Output Power
- Forced Fixed Frequency Operation and Synchronization Possible
- Load Disconnect During Shutdown
- Over-temperature Protection

And all this with only three external passive components, only one being a power inductor.

Battery

Finding a battery capable of fitting in the insole, without causing bias in the walking pattern and with enough capacity to provide a meaningful battery life is not an easy task according to the current battery technologies available in today's market.

After various searches, what became clear is that the choice of the chemistry was in fact a no-choice, being Lithium chemistry the only one to provide a large enough charge to give a significant battery life of the device at the space available in the insole.

The only two ideas where: button batteries or flexible batteries.

Company	Capacity	Form Factor	Reliability	Price	Discharge Rate
Illinois Capacitor RJD3555HPPV30M	500mAh	Button Cell 35.2mm x 5.7mm	FIG1	34.48$	0.2C
FLCB051076AAAA	97mAh	Flexible LCB 51.5 mm x 76 mm	No disclosed	No disclosed	1C
LIR3048	230mAh	30.5*5.5mm	500	$5.50	1C
GMT503533	490mAH	35mm x 5 mm	not less than 300	$10.00	0.2C
PGEB014461	200 mAH	1x61x44mm	500 cycles after 80% capacity	10.00	1C

Figure 7 Battery comparison

Flexible batteries like FLCB051076AAAA do not match in terms of capacity in front of button cell batteries. Meanwhile the two main contenders in the button battery ring are the Illinois Capacitor RJD3555HPPV30 and PowerStream

GMT503533. While in terms of price, the GMT503533 would won, its availability in the European market is non-existent. The other choice is the Illinois Capacitors, 3 times more expensive but is listed in various distributors as can be seen in figure 7:

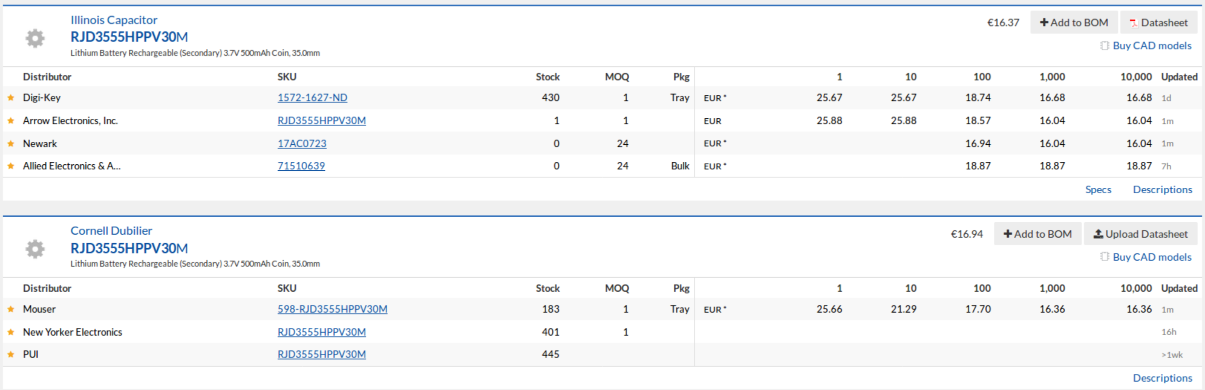

Illinois Capacitor
RJD3555HPPV30M
Lithium Battery Rechargeable (Secondary) 3.7V 500mAh Coin, 35.0mm
€16.37 Add to BOM Datasheet
Buy CAD models

Distributor	SKU	Stock	MOQ	Pkg		1	10	100	1,000	10,000	Updated
Digi-Key	1572-1627-ND	430	1	Tray	EUR *	25.67	25.67	18.74	16.68	16.68	1d
Arrow Electronics, Inc.	RJD3555HPPV30M	1	1		EUR	25.88	25.88	18.57	16.04	16.04	1m
Newark	17AC0723	0	24		EUR *			16.94	16.04	16.04	1m
Allied Electronics & A...	71510639	0	24	Bulk	EUR *			18.87	18.87	18.87	7h

Specs Descriptions

Cornell Dubilier
RJD3555HPPV30M
Lithium Battery Rechargeable (Secondary) 3.7V 500mAh Coin, 35.0mm
€16.94 Add to BOM Upload Datasheet
Buy CAD models

Distributor	SKU	Stock	MOQ	Pkg		1	10	100	1,000	10,000	Updated
Mouser	598-RJD3555HPPV30M	183	1	Tray	EUR *	25.66	21.29	17.70	16.36	16.36	1m
New Yorker Electronics	RJD3555HPPV30M	401	1								16h
PUI	RJD3555HPPV30M	445									>1wk

Descriptions

Figure 8 Battery distributors

But in case that a source of the PowerStream batteries will become available the impact in changing the batteries would be minimum being the GMT503533 smaller than the RJD3555HPPV30.

Battery Charger

For this, the choice is the MCP73831 from Microchip. MCP73831/2 devices are highly advanced linear charge management controllers for use in space-limited, cost-sensitive applications which I am already familiar with, with a low count of external components and with a 15mA to 500mA Programmable Charge Current.

Wireless power receiver

Nowadays Wireless power transceiver is synonym of Qi power transceiver due to the wide acceptance in today's smartphones and accessories market.

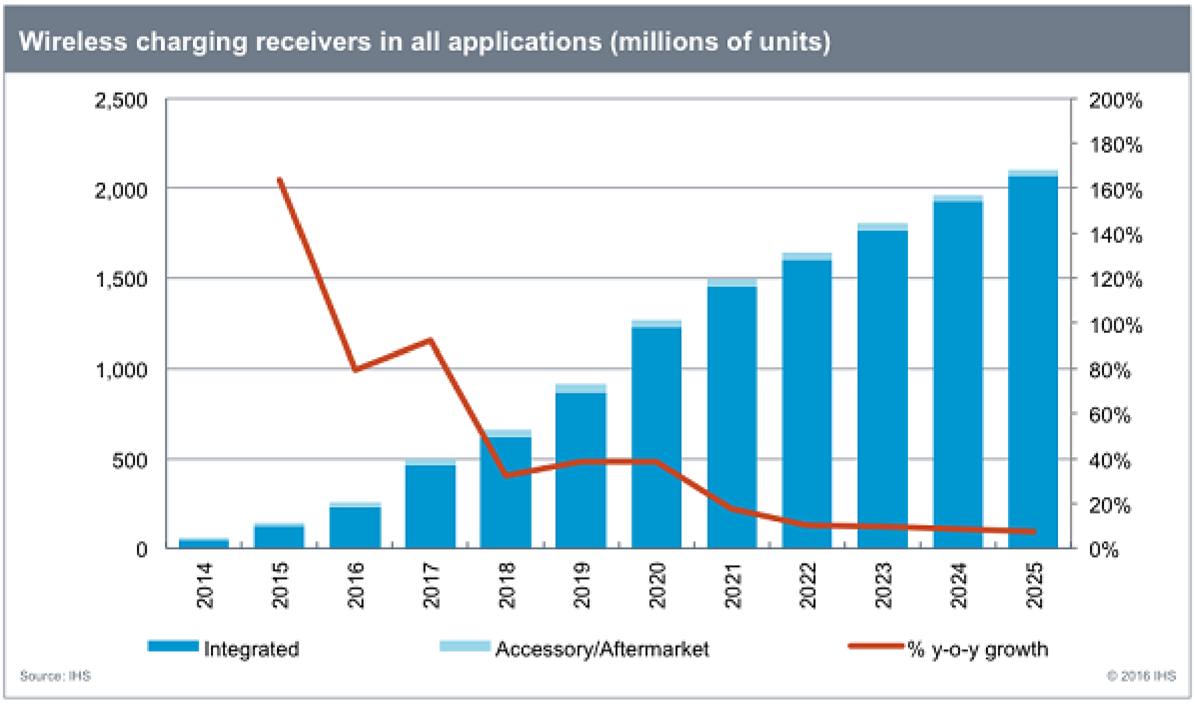

Figure 9 Wireless charging receivers projection

Almost all medium-to-high-end phones and devices incorporate a wireless transmitter or receiver and this is a growing trend as shown in the graph of level of adoption provided by The Wireless Power Consortium[11] from figure 8

For this reason, the receiver chosen is a Qi compliant receiver from the same manufacturer as the MCU SoC, STMicroelectronics. The STWLC33, in particular

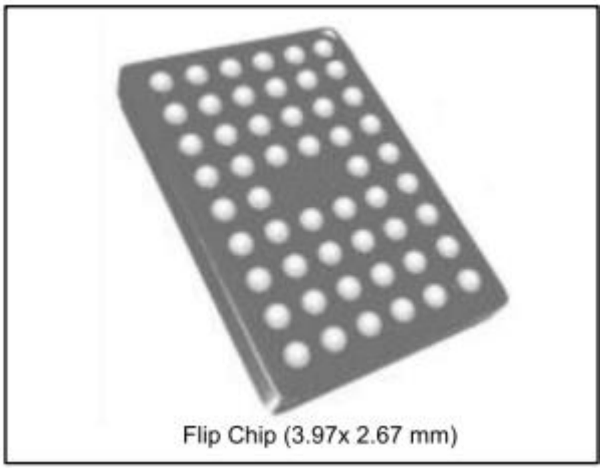

the variant STWLC33JR, encapsulates in a flip chip as shown in Figure 10.

Figure 10 Flip-chip STWLC33

A 15W receiver especially built for minimal footprint in PCB and oriented to wearable and smart-phones where, as is in the case of this insole, area is important and smaller is better.

This decision is the only miscalculation in the component selection and as will be reported later, a constant source of problems since PCB design all the way to soldering the first prototype.

Magnetic Latching Switch

The last component on this list revolves around a very simple problem, how to turn off the insole? If the insole is left working non-stop, the batteries enter a state of passivation[12] [13] may cause voltage delay after a load is placed on the cell.

But with the insole being fully enclose, adding a mechanical switch is impossible. This is the first hands-on design proposed for the insole as in a previous versions, any off-the-shelf solution was found.

It consists in a fully analog latching circuit where a momentary reed switch is transformed to a latching circuit in order to use it on the insole. A circuit and the corresponded PCB design is shown in figure 11.

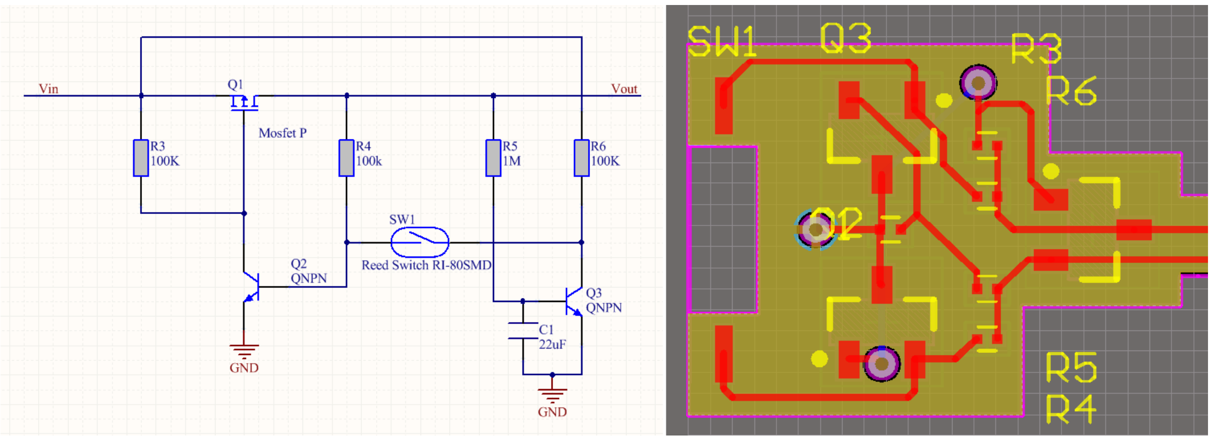

Figure 11 Custom latching circuit

This was not a good solution. Is bulky and goes completely in a different direction of the small footprint that the PCB design needed.

After many hours of searching, I found a better solution. The Melexis MLX92212LSE, a Hall effect latching circuit capable of retaining the last state without the need of a constant magnetic field as a difference to the reed switch.

If connected to the enable pin on the DC/DC could be able to turn off and on only inverting the magnetic field.

To test if it would work for that role, a sample was ordered and a quick and dirty circuit was prototype and fulfilled all the requirements for that solution.

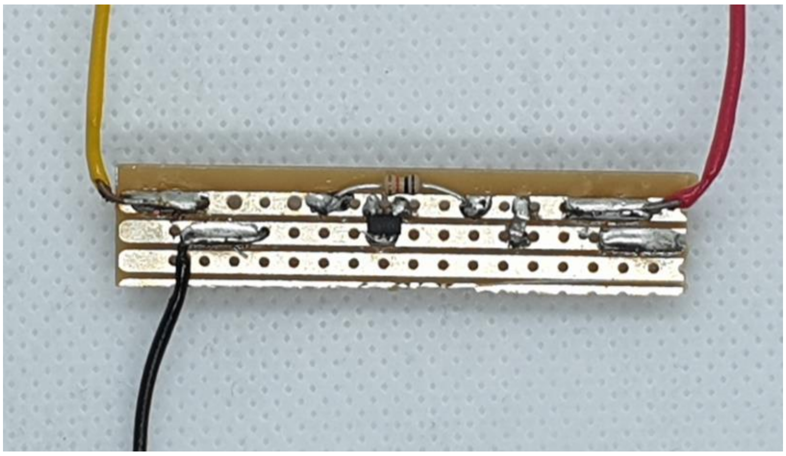

Figure 12 Melexis MLX92212LSE on protoboard

Prototyping phase

Before designing a complete PCB, it is good practice to develop some basic software to check if the selected hardware adapts well to the task. Also, in case of multidisciplinary teams where parts of the team work in hardware and another part in software, the option to have preexisting prototyping hardware for SW development makes all the development much faster.

As stated in the introduction, this is a hardware design project but the idea here is to create simple software checks, to familiarize with the structure of the project and understand "what needs to be connected where" to take it into account when creating the schematic.

Along the way and for each test there will be snippets of code using the HAL library and the GUI software STM32 CUBEMX provided by ST microelectronics.

Hello World

As for any new language, IDE or in this case microcontroller, the most obvious choice to check if all the tool-chain works is to perform a simple "Hello world!" or in case of embedded systems, a "blinky". "Blinky" is nothing more than change the state of a GPIO pin from a High-state (1) to a Low-state (0).

CubeMX is used to configure the specific MCU chosen for our project. It allows configuring the right hardware connections and to generate the FW code needed to configure the ST HAL as shown in picture 14.

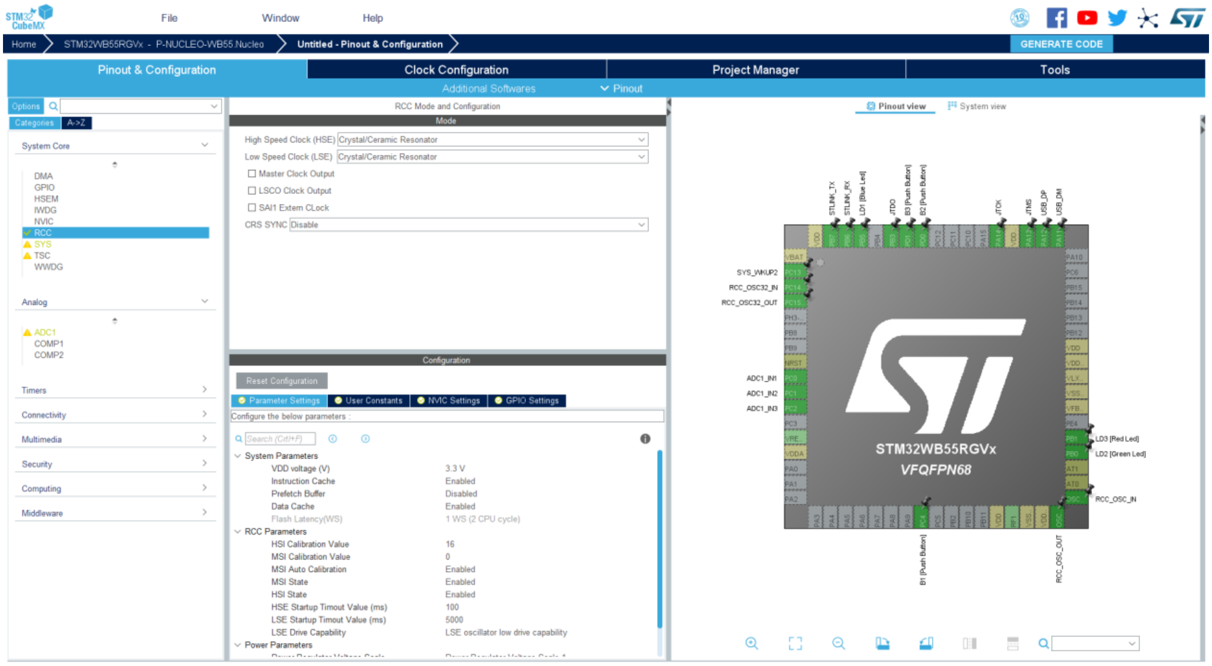

Figure 13 CubeMX STM32WB55 screenshot

With this interface, ST CubeMX generates a code template; assigns the PIN mode to the one selected; and gives a skeleton of the code with all configurations done, thus, ready to implement the custom software.

```
int main(void)
{
HAL_Init();

// LED clock initialization
LED2_GPIO_CLK_ENABLE();

// Initialize LED
GPIO_InitTypeDef GPIO_InitStruct;
GPIO_InitStruct.Pin = LED2_PIN;
GPIO_InitStruct.Mode = GPIO_MODE_OUTPUT_PP;
GPIO_InitStruct.Pull = GPIO_PULLUP;
GPIO_InitStruct.Speed = GPIO_SPEED_FAST;
HAL_GPIO_Init(LED2_GPIO_PORT, &GPIO_InitStruct);


for(;;) {
// HAL_GPIO_TogglePin(LED2_GPIO_PORT,LED_GREEN);
HAL_GPIO_TogglePin(LED2_GPIO_PORT, LED2_PIN); // Toggle the state of LED2

HAL_GPIO_TogglePin(GPIOC,GPIO_PIN_9);

HAL_Delay(400); //delay 100ms
}
}
```

Figure 14 Code snippet Blinky

With this code working, we can validate the toolchain with all dependencies correctly installed and ready to test other parts of the system.

Interface Insole-ADC

The next step in the development is to be able to read each pressure sensor from the piezo-resistive textile sensor. This step presents some unique problems, yet interesting.

For reading the analog values given by the sensors, the STM32 offers a myriad of characteristics for ADC. For example, the values could be converted and stored into a memory without any involvement of the CPU or can be read infinitely, among many other. All this is documented in the application note AN3116 ADC modes and their applications [14] where, as the title explains, provides very useful information about the ADCs in the STM32 platform.

To understand the basic configuration on CubeMX, we first rely on the manual [15] related to the board and on the AN3116 application note; and second, on what we seek to obtain. This implies knowing the following configuration concepts:

- *Clock Pre-escaler:* the frequency at which data will be captured from the ADC.
- *Scan Conversion Mode:* this mode is activated when we want to use several ADC channels.
- *Continuous Conversion Mode:* when activated, the ADC starts reading samples continuously.
- *Discontinuous Conversion Mode:* used to convert a closed set of conversions.
- *DMA Continuous Requests:* it is enabled when we want to use the DMA.
- *End of Conversion Selection:* this flag is used to determine when a conversion has been performed.
- *Number of Conversions:* determines the number of channels that will perform conversions.

The configuration chosen is shown in the figure 14:

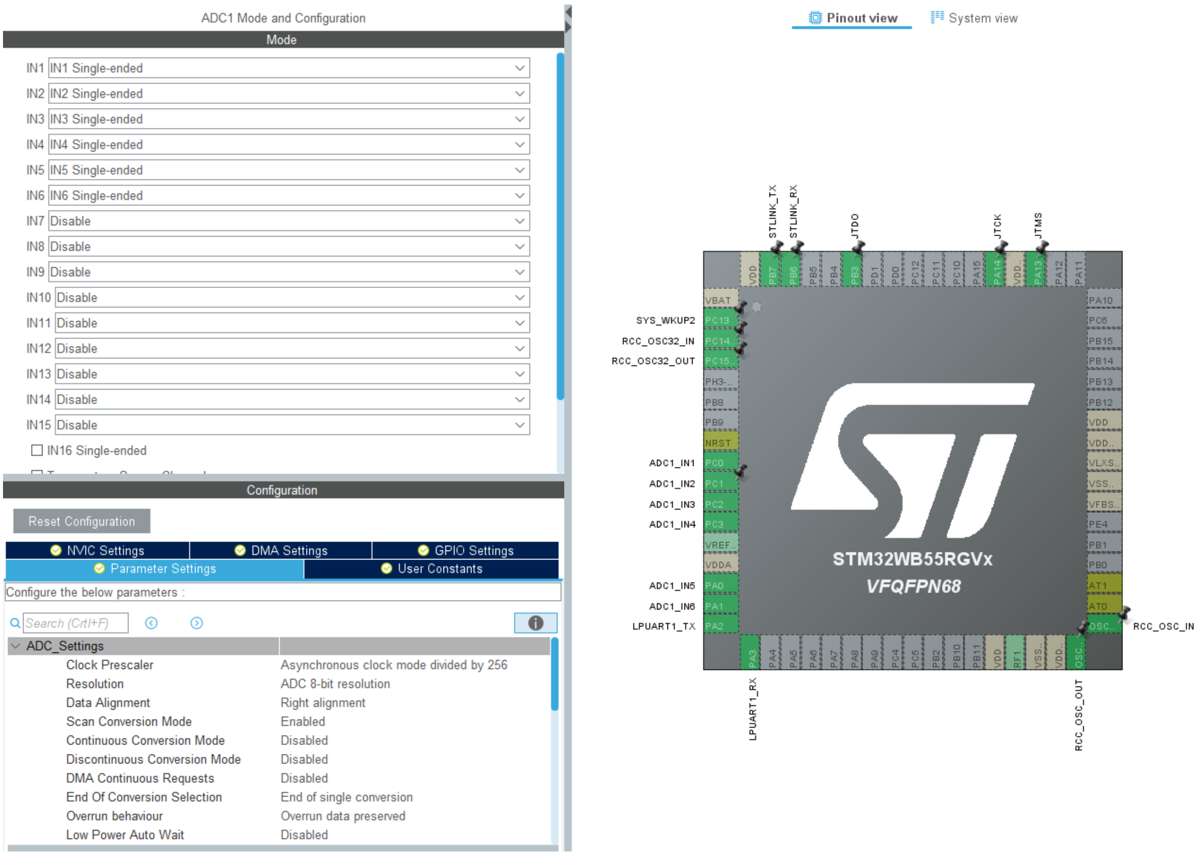

Figure 15 Cube MX configuration

Besides the configuration of the ADC, the UART port is also configured to send the data captured from the pressure sensors, back to the computer. This will allow testing the UART configuration needed for the IMU. So with one test, we are able to perform two different tasks.

As for the code, is quite a simple one (figure 15)

```
/* Orden de la plantilla derecha T44, agujas del reloj:

ADC[0] Punta Interior
ADC[1] Punta Medio
ADC[2] Talon interior
ADC[3] Talon Medio
ADC[4] Talon Exterior
ADC[5] Punta Exterior

*/
while (1)
{
  /* USER CODE END WHILE */
  /* USER CODE BEGIN 3 */
    HAL_ADC_Start(&hadc1);
  for(int i=0; i<6; i++)
  {
    HAL_ADC_PollForConversion(&hadc1, 100);
    adc[i]= HAL_ADC_GetValue(&hadc1);
  }
  HAL_ADC_Stop (&hadc1);
  printf("%d;%d;%d;%d;%d;%d; \n", adc[0],adc[1],adc[5],adc[4],adc[3],adc[2]);
  HAL_Delay(100);
}
/* USER CODE END 3 */
```

Figure 16 Code Snippet for the ADC test

Another challenging aspect of this test is the interface between the PET film odf the sensors and the functional board.

A custom PCB is the obvious choice if you want a reliable connection. But, this only fixes one of the problems. The connector footprint used in the insole sensor is a custom one (Pad Size = 0.82mm & Pitch = 1.3mm), not fabricated by any manufacturer. While this could be changed for the final product, the problem is still that any connector creates an unacceptable height for an insole and is not robust enough to survive the mechanical stress that a person's weight creates.

Another option would have been direct soldering the connector to the PCB, but PET film is not soldable. It melts way below the fusion point of any soldering paste, even with low temperature soldering paste.

The solution adopted is the use of anisotropic conductive adhesives, one of my new favorite tools. Anisotropic Conductive Film (ACF) [16] is a bonding material that uniformly distributes conductive particles with an insulating coat inside a thermosetting resin binder.

When connecting a glass substrate and IC chip, ACF is capable of establishing a connection of multiple substrate circuit electrodes simultaneously by heating and pressurizing. Particles are captured and electrically conducted on the conductor bump surface and particles that are not captured by bumps move between the terminals, but they do not conduct due to the insulating coating on particles, and the thermosetting binder provides a highly reliable adhesion.

ACF is widely used in the connection of IC chips in the flat panel displays such as high definition TVs and mobile devices. A picture is worth a thousand words:

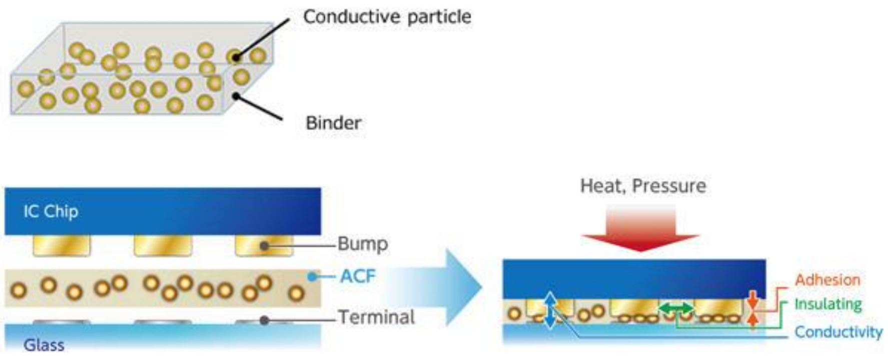

Figure 17 ACF working principle

This was the perfect solution to bond the two dissimilar material. With this solved, a custom PCB was build. It consisted in a voltage divider with a fix value of 10Kohm resistor and a V_in of 3.3v for each of the channels of the insole.

The render of the test board and the system assembled and connected to the micro-controller are shown in figures 18 and 19:

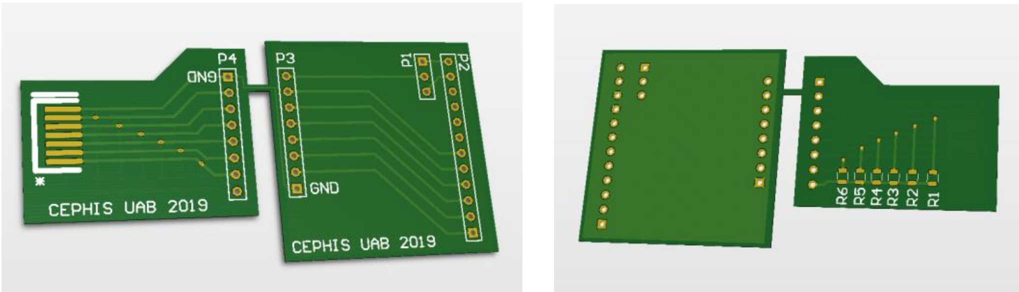

Figure 18 PCB render

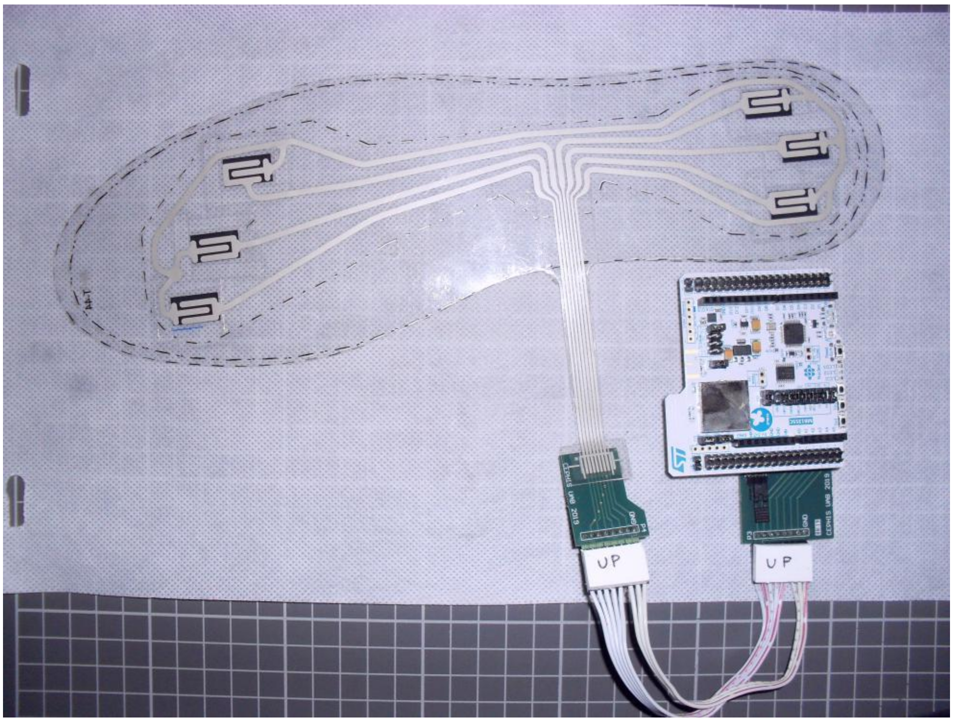

Figure 19 Test System complete

The result of the system is quite promising (figure 20), the input responds when a sensor is pressed and every channel can be captured almost at the same time.

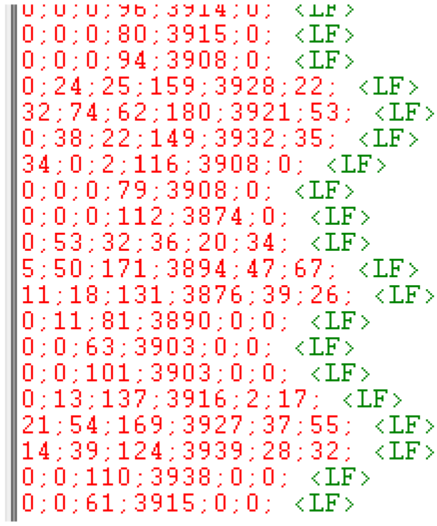

Figure 20 ADC insole results

In the captured data, something was not right. There is periodic noise in the background, like some kind of signal or like a dynamic process is repeating.

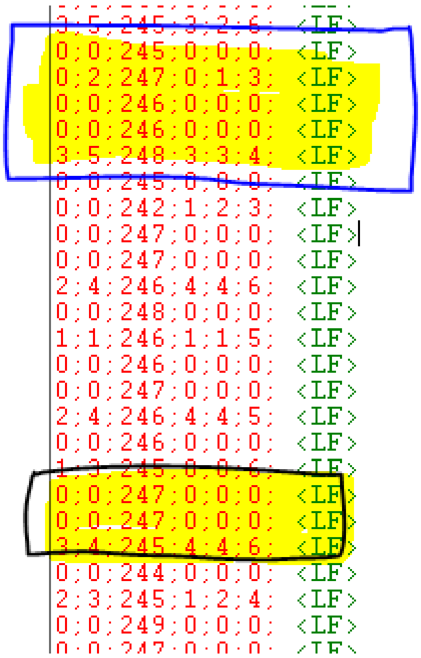

Figure 21 Cyclic error STM32

At first the assumption was a bad configuration with the ADC in the STM32 but the same noise appears using a different micro-controller, and Arduino Uno, at a different rate. Figure 21

```
0 ; 0 ; 0 ; 0 ; 0 ; 0<CR><LF>
2 ; 1 ; 0 ; 0 ; 0 ; 1<CR><LF>
6 ; 5 ; 4 ; 3 ; 2 ; 2<CR><LF>
8 ; 6 ; 1 ; 3 ; 0 ; 4<CR><LF>
6 ; 5 ; 0 ; 0 ; 9 ; 2<CR><LF>
11 ; 4 ; 4 ; 4 ; 2 ; 7<CR><LF>
4 ; 0 ; 3 ; 2 ; 5 ; 1<CR><LF>
0 ; 0 ; 0 ; 0 ; 0 ; 0<CR><LF>
2 ; 0 ; 0 ; 0 ; 0 ; 0<CR><LF>
0 ; 0 ; 0 ; 0 ; 0 ; 0<CR><LF>
0 ; 0 ; 0 ; 0 ; 0 ; 0<CR><LF>
0 ; 0 ; 0 ; 0 ; 0 ; 0<CR><LF>
0 ; 0 ; 0 ; 0 ; 0 ; 0<CR><LF>
0 ; 0 ; 0 ; 0 ; 0 ; 0<CR><LF>
0 ; 0 ; 0 ; 0 ; 0 ; 0<CR><LF>
0 ; 0 ; 0 ; 0 ; 0 ; 0<CR><LF>
0 ; 0 ; 0 ; 0 ; 0 ; 0<CR><LF>
2 ; 0 ; 1 ; 0 ; 0 ; 1<CR><LF>
4 ; 0 ; 1 ; 1 ; 1 ; 2<CR><LF>
9 ; 1 ; 4 ; 4 ; 2 ; 1<CR><LF>
14 ; 2 ; 0 ; 10 ; 0 ; 0<CR><LF>
10 ; 1 ; 5 ; 5 ; 1 ; 1<CR><LF>
6 ; 8 ; 1 ; 0 ; 3 ; 3<CR><LF>
3 ; 4 ; 1 ; 0 ; 0 ; 1<CR><LF>
2 ; 0 ; 0 ; 0 ; 0 ; 0<CR><LF>
0 ; 0 ; 0 ; 0 ; 0 ; 0<CR><LF>
```

Figure 22 Cyclic error Arduino Uno

This issue was informed to Sensingtex, that as of yet is unable to find a reason for this behaviour.

BLE test

For the test of making the BLE 5 work, the difficulty is in understanding all the stack associated to Bluetooth provided by ST microelectronics. Adding to that that the STM32WB chip is just released to the market, the documentation is still scarce by the company and adding even more than the programming of micro-controllers, although it is not strange to me, it is not at all my specialty.

This is why I decided to attend a course presented by ST in Grenoble. Unfortunately, the course is aimed at French-speaking engineers being given entirely in French. When I got in touch with them, they kindly sent me the courses in English with examples of how to activate Bluetooth in the development plate.

With these examples, the code was loaded in the micro-controller and by means of its android app (figure 22). I verified that the code works by sending the value of the internal temperature sensor of the MCU.

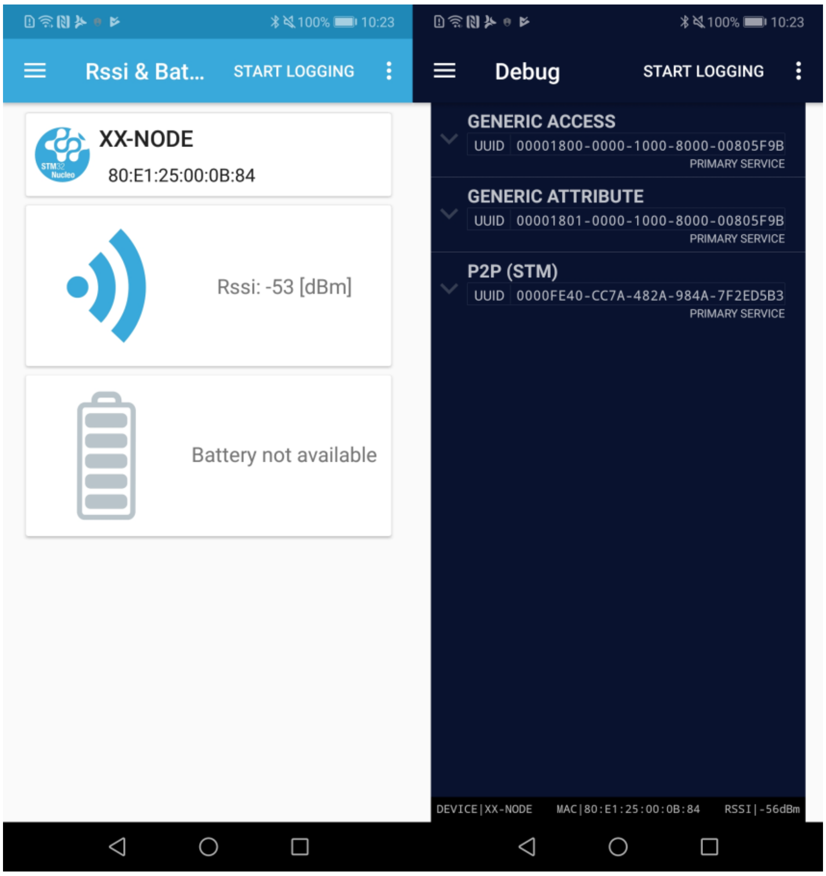

Figure 23 BLE test

Miniaturization

The results of the different tests done with the prototyping boards produced satisfactory results. The next step is to develop a full PCB design implementing all the knowledge acquired in the test and produce a highly integrated solution being capable to be encapsulated in the insole. As it is well know, the PCB is physical representation of the interconnection of the electrical signals. In short, the solution must integrate all technologies shown in picture 24 in the smallest possible PCB

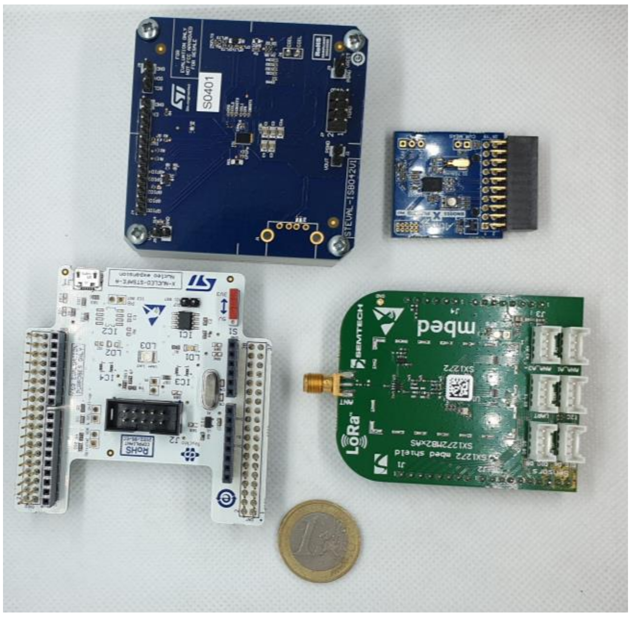

Figure 24 Technology to fit in the PCB

To create this PCB the software package use is Altium Designer, one of the most popular of the high-end PCB design software packages on the market today. It is developed and marketed by Altium Limited. It includes schematic entry, PCB module, and auto-router and differential pair routing features. It supports track length tuning and 3D modeling.

Also Altium Designer includes tools for all circuit design tasks: from schematic and HDL design capture, circuit simulation, signal integrity analysis, PCB design, and FPGA-based embedded system design and development. In addition, the Altium Designer environment can be customized to meet a wide variety of users' requirements.

Footprint Generation

Footprints define the physical interface between the PCB and the component (the land pattern) and include documentation information (outline, polarization mark, reference, ...). The land pattern is either directly taken from the datasheet, or derived from the components dimensions (including tolerances) via industry standards (most likely the suggested land pattern is derived from such a standard as well).

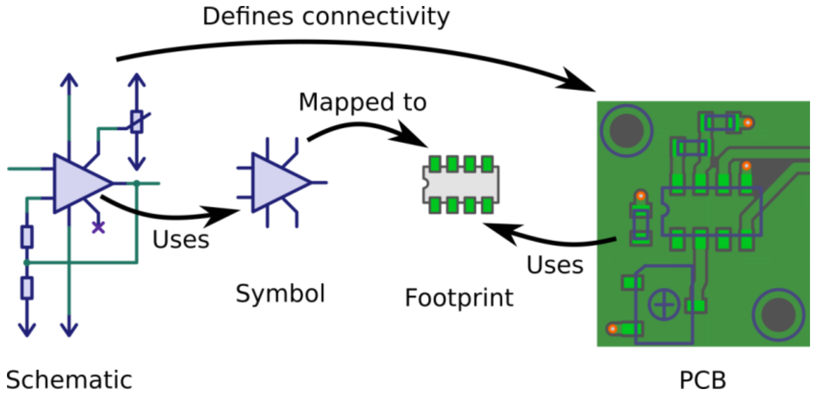

Figure 25 PCB explanation

At least, it needs to contain all pads (connection points) to solder the component (shape and size/position of the pad should meet what is given in the datasheet). Pads define what features appear on copper, mask and paste layers: copper is the area covered by copper metal; mask gives the cutout in the solder mask layer; and paste is the cutout of the solder paste stencil used for reflow soldering.

Sadly, Altium Designer does not provide the footprints for almost any component. The market has millions of components with a lot more being created every day. It is not feasible for any company to maintain a database with such a large data-set.

For this, we have 3 methods:

- Generated the footprints by hand, calculating the distances and other feature with the information in the datasheet
- Make use of the wizard included in Altium Designer and with some minimal information, it generates all the features

- Import the footprint directly from the reference design. Using an industry standard like Altium, allow that since ~95% of design are done using Altium.

First design

The next step is to create the schematics of the system.

One note for people without experience is that, even this process is a linear one, there is a lot of back and forth jumping between steps in the design process. Missing components that you notice when you are designing the schematic or the PCB. Changes in the requirements of the project, etc.

To no clutter the schematic pad and create a legible scheme, the full schematic is divided in three sheets based on the amount of components needed:

- Power section
- MCU section
- LoRa Section

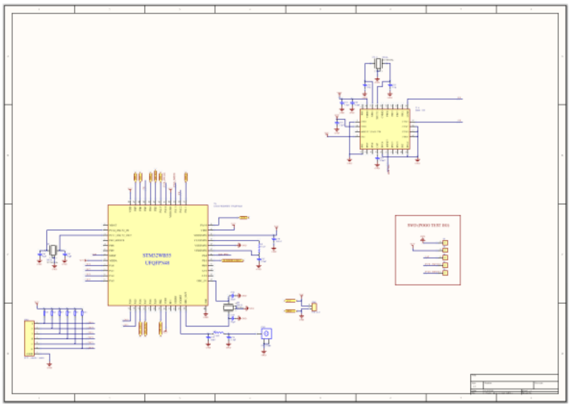

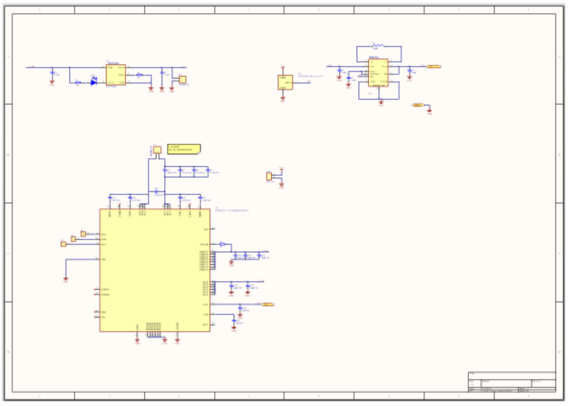

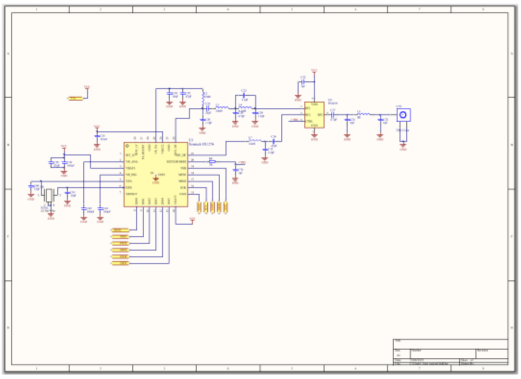

Figure 26 Schematic Thumbnails

One of the first evolutions of the PCB is to create a floor-plan and discuss the pros and contras of the design. Later, d

The annex 01 contains the full scale schematics to visualize better the details.

Different versions will be created along the design process while doing estimations and decisions about how the PCB final design would be.

One of the early floorplans called for creating two different PCB, one for the right foot and another one for the left foot, as shown in Figure 27, the design would have been symmetric and double time to design the PCBs and double the cost in production.

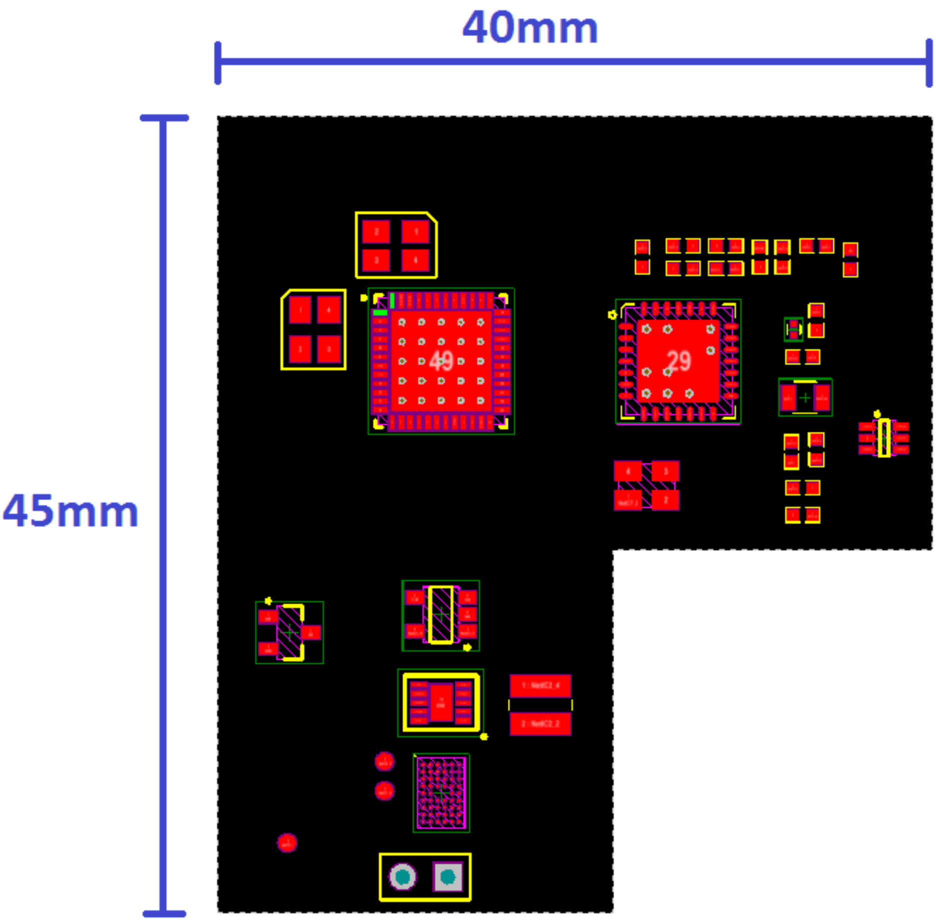

Figure 27 Floorplan

This is a very rough initial design, with a lot of missing features like the full spatial IMU, the sensor connector or the antenna U.FL connectors. Also, the rigid-flex technology is missing on this prototype.

Rigid-Flex PCB

Rigid Flex PCB are printed circuit boards highlighted by both rigid and flexible areas that make them ideally suited for a wide range of applications.

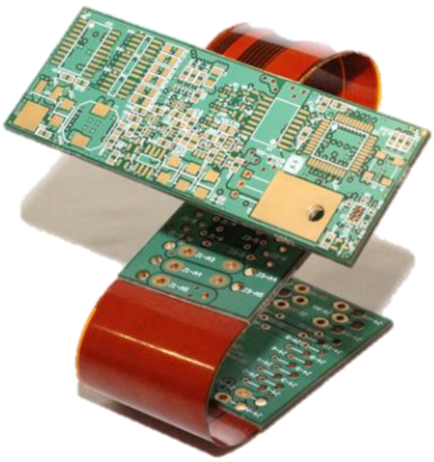

Figure 28 Rigid-flex example

The typical rigid-flex PCB circuit includes two or more conductive layers that comprise either flexible or rigid insulation material between each one - the outer layers may have either exposed pads or covers. Conductors are found on the rigid layers, while plated through-holes are found in both the rigid and flexible layers.

The advantages of this kind of technology are:

- ❖ Less space required due to three-dimensional wiring.
- ❖ Elimination of additional components such as connectors and cables.
- ❖ Improved signal transmission through elimination of cross-sectional changes to conductors (connectors, cable, solder connections).
- ❖ Weight reduction.
- ❖ Considerably improved reliability of the entire system (a homogeneous unit is considerably more reliable than one with connectors and cable).

In the case of this design, also provides a flexible point to adapt a rigid material to the natural movement of the feet while walking or running thus not creating a bias.

To separate the PCB, we implement the separation the same as in the architecture explanation, Power PCB on one side, Logic PCB on the other.

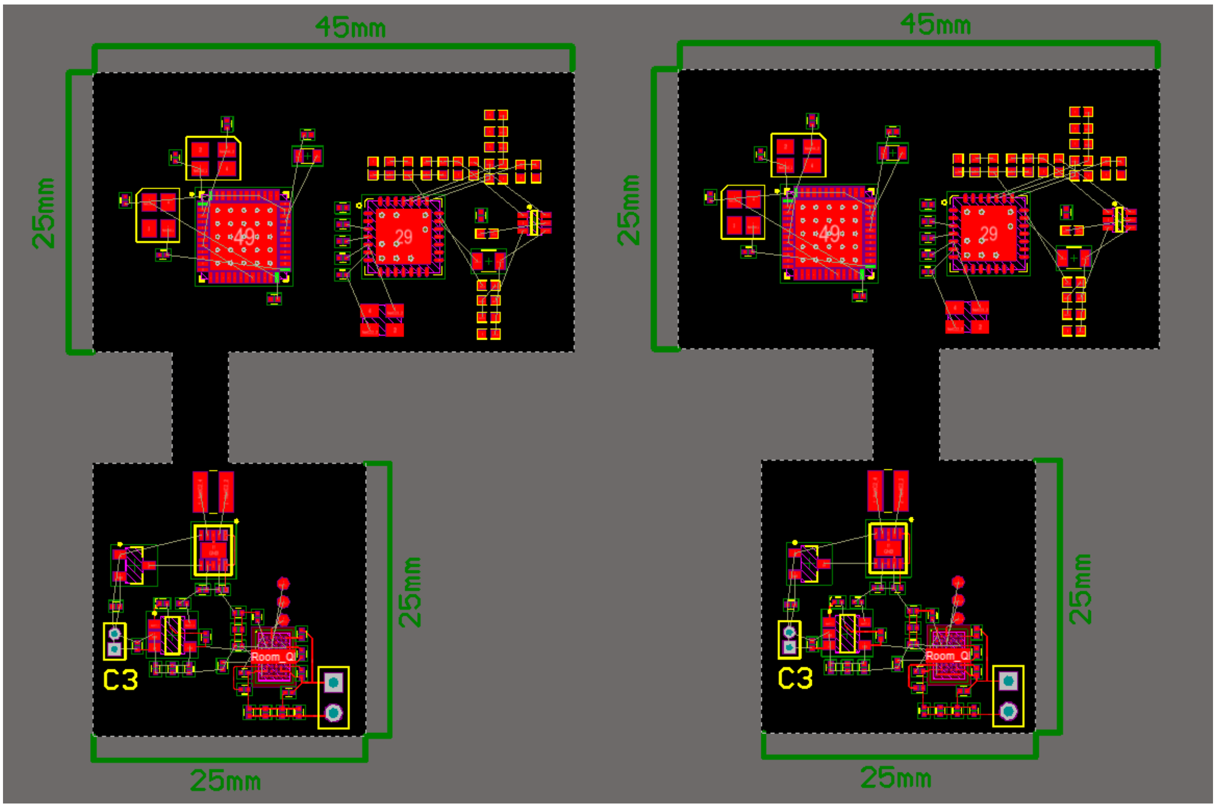

Figure 29. Further PCB floorplans

At the left of Figure 29, there is the evolution of the first floorplan, with its dual PCB one for each insole, and at the right, there is the change made to the rigid-flex being centered to create only one design.

The design evolved, implementing the traces, adding components and shifting all of them around to create the smallest PCB design possible. In lots of cases, PCB design compares to puzzle solving or geometrical problems. After some more iterations, a well evolve design is completed.

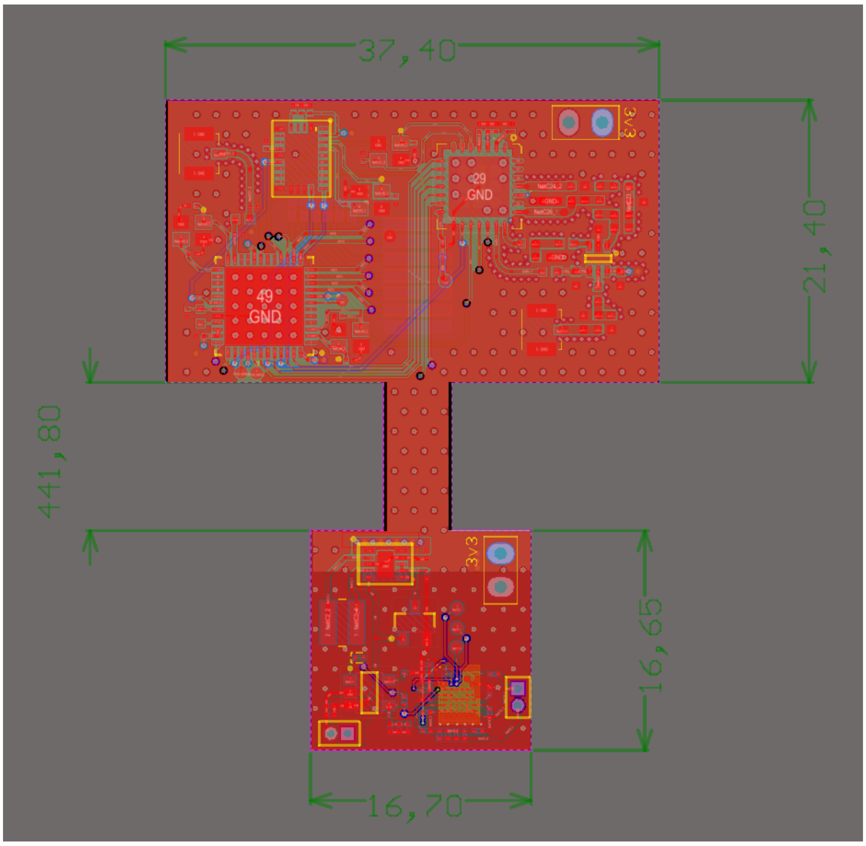

Figure 30 Final Stage

A more detailed render can be seen in annex 02.

As can be seenFigure 30 shows that the Power board is reduced almost half in terms of area and the Logic board is smaller with more components on it. Further optimizations are possible both in terms of space and in terms of cost. Creating a small PCB is only a matter of time, but this miniaturization comes with a cost in terms of price charged by the manufacturer. Elements as micro-via are sometimes required while you can work with the company to reduce cost with minimal changes in the PCB. For example, Figure 31 seems to be the same design.

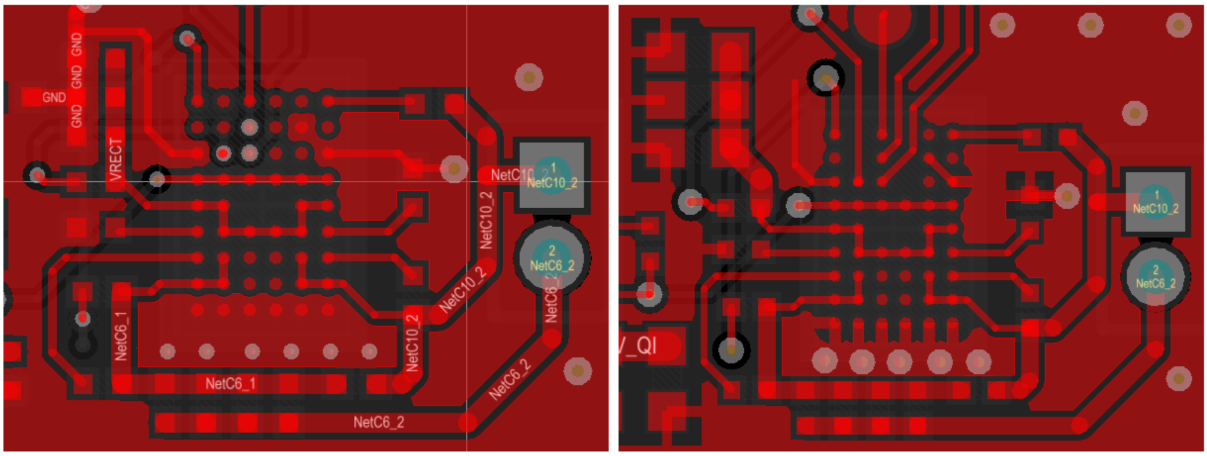

Figure 31. Design changes due to interations with the PCB manufacturer

As stated in the Architecture chapter, the Qi receptor is the component that caused the most problems, in this case because the pitch of the footprint pads.

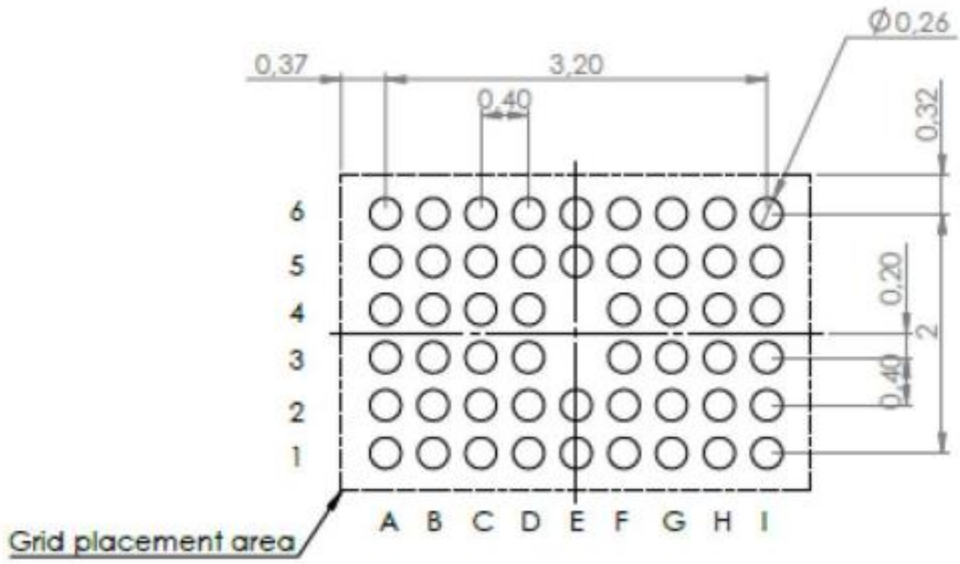

Figure 32 STWLC33 dimensions

Working at this size is not a small feat. Usually this size is reserved for HDI (High Density Interconnection) designs that need to include lots of components in a small space. The use of micro-vias is usually associated with HDI design.

μ -Vias

A micro-via is obviously a smaller via (an interconnection between layers of the PCB). As a reference, most people consider micro-vias to be a via with a diameter lower than 150 μm. These tiny holes are drilled by lasers, a process that is constantly being improved thanks to Ultrafast UV Lasers [17] that drill faster and more precise than current CO_2 lasers. New advances in laser drilling techniques could reduce micro-vias down to 15 μm. The lasers involved can only drill through one layer at a time. However, manufacturers can make through micro-vias by drilling them separately in multiple layers and stacking them.

Micro-vias have a lower potential for manufacturing defects than normal vias. This is because laser drilling does not leave any material behind the drilled holes. But micro-vias have the same risks as normal vias when it comes to plating and reflow soldering.

This manufacturing process also need to tickle down to smaller manufacturers that does not deal with very large volume productions and their investment costs can be problematic. In the present case, to have access to the inner pads of the component the only solution is to use micro-vias in the same pad, as shown in Figure 33.

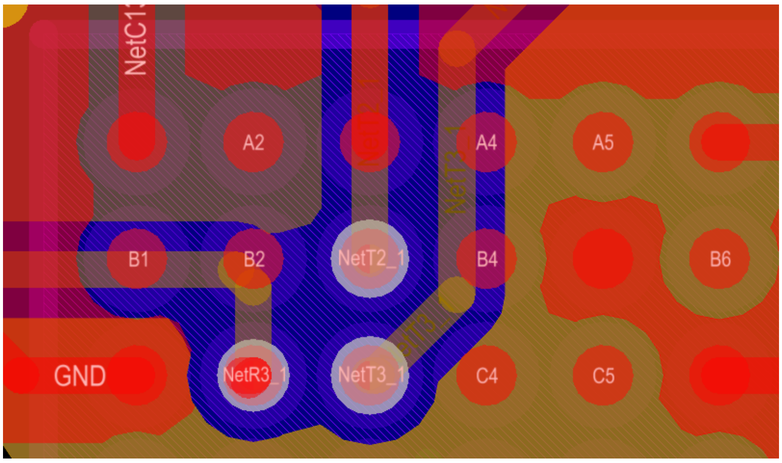

Figure 33. In pad micro-via.

Is true that this design is a first iteration of a prototype, so cost is not as important as if we were in a production run, where every penny counts. To create a work around these micro-vias, we decided, together with the manufacturer, to eliminate some of the pads that are not used in the component and route a line through them. This is a bit risky since we are fully convinced that the silks-screen (a dielectric layer build on top of the PCB to avoid oxidation and what gives the characteristic green color to the PCB) will resist a reflow soldering process. With this modification, the price per PCB is reduced a 25% being the first offer 7.73€ and after the modifications 5.85€ as highlighted in Figure 34.

Codi : SERENE_FAB_FILES	Referència : Email 13/05/2019	Codi Lab : 109-999-18

Pos.	Servei	Quantitat ofertada	Acabat	Preu Unitari	Despeses	Termini
1	Proto Express	min. 4	Im.Ag	11,59 €	GRP 1.112,00 €	5½ dies laborables
2	Proto Standard	min. 4	Im.Ag	7,73 €	GRP 741,00 €	9 dies laborables

- Oferta realitzada pel subministrament en un panell de 2 unitats separades per fresat de mides 121,60x 57,40 mm amb marc perimetral.

Codi : SERENE_FAB_FILES	Referència : Email 13/05/2019	Codi Lab : 109-999-18

Pos.	Servei	Quantitat ofertada	Acabat	Preu Unitari	Despeses	Termini
1	Proto Express	min. 8	Im.Ag	9,88 €	GRP 1.112,00 €	5½ dies laborables
2	Proto Standard	min. 8	Im.Ag	6,59 €	GRP 741,00 €	9 dies laborables

- Aquesta oferta substitueix a l'anterior, de número 2291/19 i data 14/ 5/19.
- Oferta realitzada pel subministrament en un panell de 4 unitats separades per f resat de mides 121,60x 97,80 mm amb el marc perimetral ja contat.

Codi : SERENE_FAB_FILES	Referència : Email 17/05/2019	Codi Lab : 109-999-18

Pos.	Servei	Quantitat ofertada	Acabat	Preu Unitari	Despeses	Termini
1	Proto Express	32	Im.Ag	8,78 €	GRP 980,00 €	4½ dies laborables
2	Proto Standard	32	Im.Ag	5,85 €	GRP 653,00 €	8 dies laborables

- Les vies cegues entre capes 1-2 i capes 3-4 es consideren com a microvies làser de diàmetre 0,1mm, de tal manera que només cal un procés de metal·lització de les vies.
- Aquesta oferta substitueix a l'anterior, de número 2311/19 i data 15/ 5/19.

Figure 34 Cost reduction

Another issue I had to deal with is the great number of vias connected to ground spread through the whole PCB. This is a technique called via stitching and via shielding. Via stitching is used to tie together larger copper areas on different layers, in effect creating a strong vertical connection through the board structure, helping maintain a low impedance and short return loops. Via stitching ties copper areas that might otherwise be isolated from their net as shown in Figure 35.

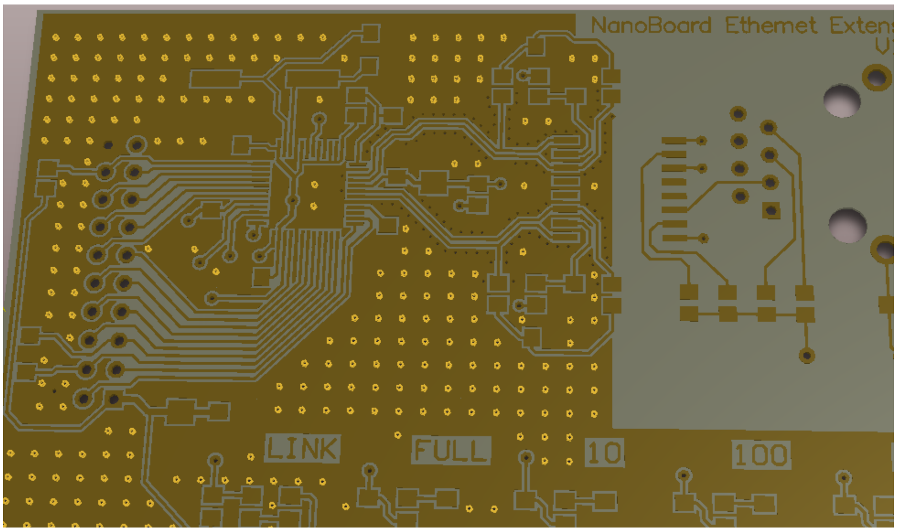

Figure 35 Via stitching

Via shielding has a different function. Specially in RF designs, it is used to help reduce crosstalk and electromagnetic interference in a routed wire carrying an RF signal. A via shield, also known as via fence or picket fence, is created by placing one or more rows of vias alongside the signal's route path as shown in Figure 36.

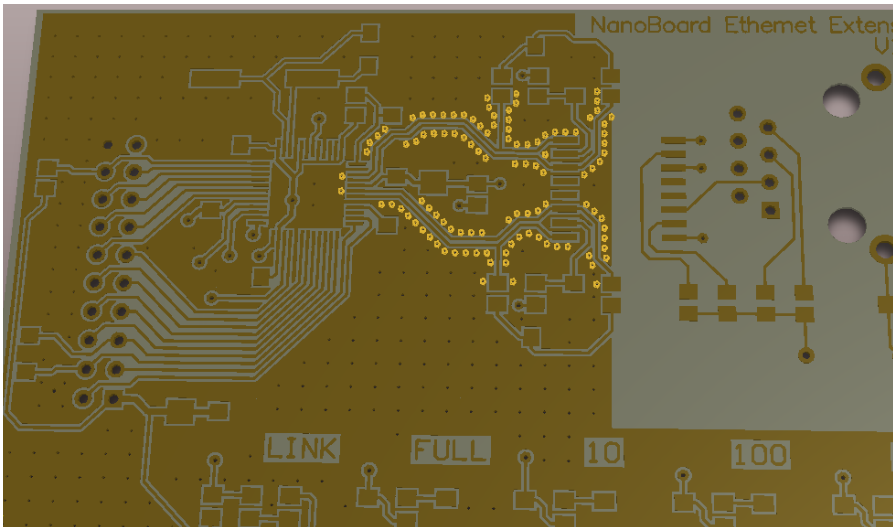

Figure 36 Via shielding

As a result, the manufacturer created the PCB shown in figure 37 from the Gerber files we sent him as a result of our PCB design.

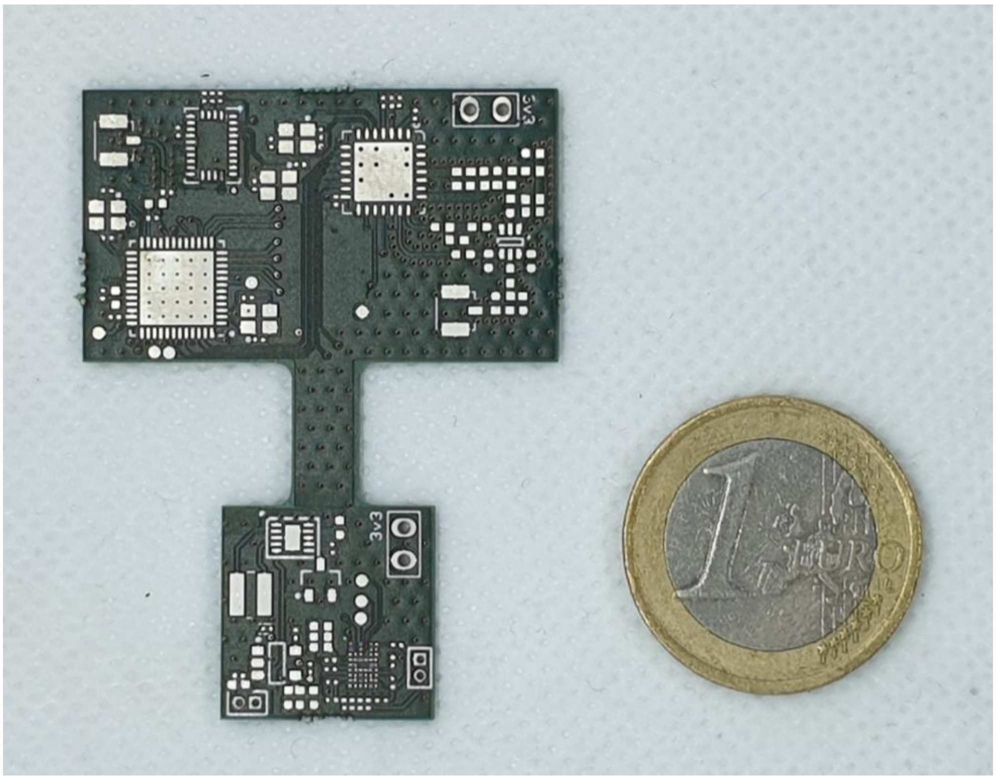

Figure 37 PCB real version

Prototype Assembly

After building the PCB, we have to mount the components onto the board before testing if the prototype is working. It is possible to subcontract companies to mount these components on the PCB. A machine will mount all the components at once, without caring if the 3.3v rail is working or if there is some short circuit.

Anyway, it is usually better to do an incremental mounting and testing of the system for the first prototypes. This is usually better done at the own facilities since it is prohibitive in terms of subcontracting budget. Furthermore, maybe the footprint is not exactly correct and some adjustments are needed when soldering the components. Anyway, both in the PCB design and in the mounting it is important to contact the industry that will finally mount the prototypes for series production.

Bill of Materials

Prior to solder the components we need first to buy those components. For that, a Bill of Materials is created at the end of the PCB design process.

One of the advantages of using a software package as Altium is the option to automatize this process. For boards with a small amount of components, 10 to 20, doing a list by hand is possible, but this prototype has more than 50 components, all of them different, that need to be solder in the right spot. Figure 38 shows the list of components and the work done. In annex 03 is a expanded view.

1	Comment	Description	Designator	Footprint	Quantit	Value	SKU	Price	Distributor	
2	Cap	Capacitor SMD	C1, C2	rlc_402_smd	2	10uF	2611904	0,177|@10u	Farnell	
3	Cap	Capacitor SMD	C3	rlc_402_smd	1	4.7uF	2688503	0,19|@10u	Farnell	
4	Cap	Capacitor SMD	C4	RLC_0201_SMD	1	4.7uF (Cambiado por 1uF	2672085	0,139|@10u	Farnell	
5	Cap	Capacitor SMD	C5	RLC_0201_SMD	1	0.1uF	2528750	0,133|@10u	Farnell	
6	Cap	Capacitor SMD	C6, C7, C8, C9	RLC_0201_SMD	4	100nF/50v (cambiado de	2611885	0,0238|@10u	Farnell	
7	Cap	Capacitor SMD	C10	RLC_0201_SMD	1	3.9nF/50v (cambiado de	81-GRM33R61E392KA12D	0,014|@10u	Mouser	
8	Cap	Capacitor SMD	C11, C14	RLC_0201_SMD	2	15nF/10v	81-GCM033R71A152KA3D	0,04|@10u	Mouser	
9	Cap	Capacitor SMD	C12, C13	RLC_0201_SMD	2	47nF/50v (cambiado de	81-GRM033R71E472KE4D	0,017|@10u	Mouser	
10	Cap	Capacitor SMD	C15, C16, C17, C18,	rlc_402_smd	5	10uF/25v (cambiado de 2	GRM155C80J106ME11D	0,14|@10u	Mouser	
11	Cap	Capacitor SMD	C20, C21	RLC_0201_SMD	2	1uF/10v	581-0201ZD105MAT2A	0,148|@10u	Mouser	
12	Cap	Capacitor SMD	C22, C36	rlc_402_smd	2	1nF	77-VJ0402Y102KXQCBC	0,192|@1u	Mouser	
13	Cap	Capacitor SMD	C23	rlc_402_smd	1	1.2pF	581-0101YA1R2BAT2A	0,281|@10u	Mouser	
14	Cap	Capacitor SMD	C24	rlc_402_smd	1	10nF	581-0402ZC103MAT2A	0,031|@10u	Mouser	
15	Cap	Capacitor SMD	C25, C34	rlc_402_smd	2	47pF	80-C0402C470J8G	0,178|@10u	Mouser	
16	Cap	Capacitor SMD	C26	rlc_402_smd	1	33pF	80-C0402C330K8G	0,173@10u	Mouser	
17	Cap	Capacitor SMD	C27, C28	rlc_402_smd	2	4.7pF	80-C0402C479K8G	0,169|@10u	Mouser	
18	Cap	Capacitor SMD	C29	rlc_402_smd	1	1.8pF	81-GJM0225C1C1R8CB1L	0,085|@10u	Mouser	
19	Cap	Capacitor SMD	C30	rlc_402_smd	1	1.5pF	81-GJM0225C1C1R5WB1L	0,196|@10u	Mouser	
20	Cap	Capacitor SMD	C31, C32	rlc_402_smd	2	0pF	No mounted	0		
21	Cap	Capacitor SMD	C33	RLC_0201_SMD	1	100nF	81-GRM033C71A104KE4D	0,053|@10u	Mouser	
22	Cap	Capacitor SMD	C35	rlc_402_smd	1	3.3pF	81-GRM0225C1C3R3CA3L	0,045|@10u	Mouser	
23	Capacitor	Capacitor SMD	C38	RLC_0201_SMD	1	47pF	2576363	0,0184|@10u	Farnell	
24	Capacitor	Capacitor SMD	C39, C42, C43, C4	RLC_0201_SMD	5	100nF	81-GRM033C71A104KE4D	0,053|@10u	Mouser	
25	Capacitor	Capacitor SMD	C40, C41	RLC_0201_SMD	2	15pF	81-GCM0335C1E150JA6D	0,044|@10u	Mouser	
26	Capacitor	Capacitor SMD	C44, C45, C48, C4	RLC_0201_SMD	4	22pF	81-GJM0335C0J220JB1D	0,065|@10u	Mouser	
27	Capacitor	Capacitor SMD	C47	RLC_0201_SMD	1	4.7uF	81-GRM035R60J475ME5D	0,295|@10u	Mouser	
28	Capacitor	Capacitor SMD	C50	RLC_0201_SMD	1	0.8pF	81-GRM0335C1ER80BA1D	0,017|@10u	Mouser	
29	Capacitor	Capacitor SMD	C51	RLC_0201_SMD	1	0.3pF	81-GJM0335C1ER30BB01	0,071|@10u	Mouser	
30	Capacitor	Capacitor SMD	C52, C53	RLC_0201_SMD	2	6.8p	2906255	0,193|@10u	Farnell	
31	Capacitor	Capacitor SMD	C54, C57	RLC_0201_SMD	2	4.7pF	2434626	0,0183|@10u	Farnell	
32	Capacitor	Capacitor SMD	C56	RLC_0201_SMD	1	120nF (cambio a 150nF)	2526217	0,256|@10u	Farnell	
33	UFL Conn	UFL Hirose U.FL-R-SMT-1(10)	CN1, CN2	UFL Conn	2		1688077	0,816|@10u	Farnell	
34	PIN_1x2	Tira de pines 2 contactos	CN4, CN5	PIN_1x2	2	NO mounted	No Mounted			
35	MCP73831	Miniature single-cell, Li-ion/Li-Po charge	IC1	MCP73831	1		1332158	0,484|@10u	Farnell	
36	TSP6303x	TSP6303x Buck/boost converter single	IC2	TPS6303x	1		1689433	1,82|@1u	Farnell	
37	LPS3015	LPS3015 Shielded SMT Power Inductor	L1	LPS-3015	1	1.5uH	2408018	1,55|@1u	Farnell	
38	Inductor	Inductor	L2	rlc_402_smd	1	33nH	810-MLG0402Q33NJT000	0,214|@10u	Mouser	
39	Inductor	Inductor	L3, L7	rlc_402_smd	2	10nH	810-MHQ0402PSA10NHT	0,074|@10u	Mouser	
40	Inductor	Inductor	L4	rlc_402_smd	1	6.2nH	810-MLG1005S6N2HT000	0,038|@10u	Mouser	
41	Inductor	Inductor	L5	rlc_402_smd	1	0R	755-SFR01MZPJ000	0,056|@10u	Mouser	
42	Inductor	Inductor	L6	rlc_402_smd	1	10uH	81-LQW15DN100M00D	1,81|@10u	Mouser	(futuro cambio empaquetado por uno mayor 0603)
43	Inductor	Inductor	L8	rlc_402_smd	1	2.7nH	810-MLG1005S2N7CT000	0,038|@10u	Mouser	
44	LED	LED	LD1	0201 - LED	1	LED	696-SMLLX0201UPGCTR	0,242@10u	Mouser	
45	MHDR1X2	Header, 2-Pin	P1, P2	MHDR1X2	2	Paso 1,27mm	No mounted	No mounted		
46	XTAL	Crystal with GND pins	Q1, Q2, UX_1	ND_2520	3	32.768 KHz	1674695	1,41|@10u	Farnell	
47	XTAL	Crystal with GND pins	Q3	ND_2520	1	16MHz	2469941	0,722|@10u	Farnell	
48	Resistor	Resistor SMD - IEC symbol version	R1	RLC_0201_SMD	1	1K	603-AC0201FR-071KL	0,048|@10u	Mouser	
49	Resistor	Resistor SMD - IEC symbol version	R2	RLC_0201_SMD	1	330	652-CR0201-JW-331GLF	0,083|@10u	Mouser	
50	Resistor	Resistor SMD - IEC symbol version	R3	RLC_0201_SMD	1	30	71-CRCW020130R0FNED	0,063|@10u	Mouser	
51	Resistor	Resistor SMD - IEC symbol version	R4	rlc_402_smd	1	1K	755-SFR01MZPJ102	0,056|@10u	Mouser	
52	Resistor	Resistor SMD - IEC symbol version	R5, R6, R7, R8, R9	rlc_402_smd	6	10k	755-SFR01MZPF1002	0,069|@10u	Mouser	
53	test point	Punto de testeo 1mm	T1, T2, T3, T4, T5, T	test_point	8	#################	###################	#############################		
54	MLX92212LSE-AAA-(	3-Wire Hall Effect Latch	U1	SOT23	1	#################	482-92212LSEAAA000RE	0,777|@1u	Mouser	
55	STWLC33_!!!!PAD RE	Multi-mode Qi/AirFuel inductive wireless	U2	STWLC33 - PADS DELE	1	#################				
56	Semtech SX1276	Semtech SX1276	U3	vqfn28_6x6mm	1		947-SX1276IMLTRT	7,04|@1u	Mouser	
57	STM32WB55XX_UF(	SoC BLE STM32	U4	STM32WB55xx UFQFPN	1		#################	########################		
58	PE4259	RF Switch	U9	Peregrine PE4259	1		#################	########################		
59	BNO_055	IMU	U_4	BNO_055	1		262-BNO055	9,25|@1u (8.32|@10u	Mouser	

Figure 38 BoM

With the BoM ordered and delivered to the procurement facilities, we will start soldering the components after their arrival. The first step is to validate that the power rail of 3.3v works correctly.

Soldering and Test Plan

Soldering and testing the prototype, with its different subsystems, requires a tets plan. It will keep track of what works, what does not work and what needs to be fixed for a second PCB generations. The test plan is de description of the series of tests that must be done to ensure that the system works. In annex 04 there is the full document, with annotations of the test done.

As stated before, doing an iterative soldering and testing has the benefits of detecting errors like the one in the hall latching switch. We detected that the footprint was wrongly implemented without connecting its ground to the same ground of the voltage regulator and thus not supplying power to it. We can correct that error by using wire wrapping. After that, the prototype is working, supplying the 3.3v and charging from the regulator.

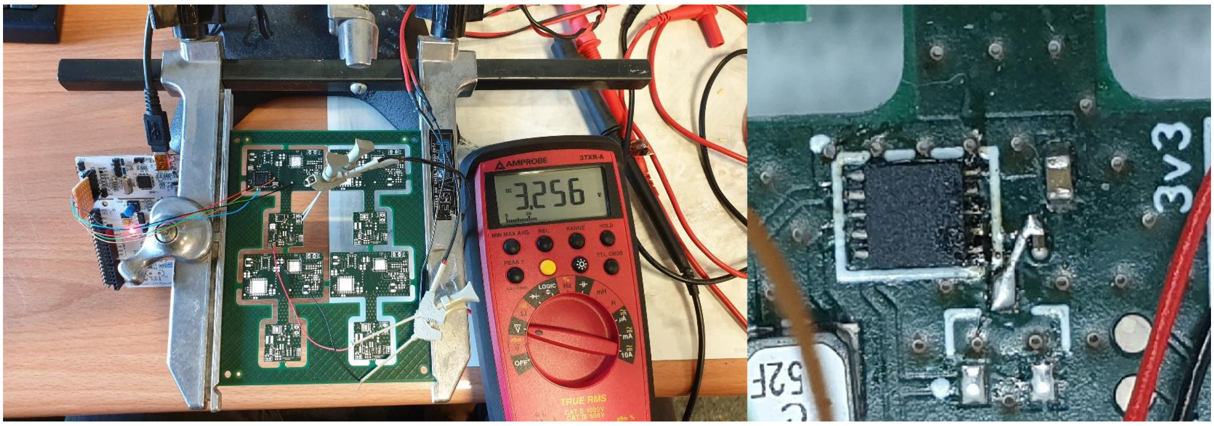

Figure 39 Prototype Working and close-up of the modifications

For the Qi receiver, the component was not available in any distributor because the company producing it has stopped production during half a year, even being only 1 year old. Thus, it has been decided not to mount it and wait for a second prototype to change the Qi receiver.

After testing the power board, the next step is to mount the logic board, using the same iterative process. For the logic board, the first step is to solder the MCU and all the XTAL that allow its operation.

Figure 40 Close Up of the MCU and other components.

As shown in Figure 40, five wires have been soldered in test pads around the board. This test pads are the programming connection that using a Serial Wire Debug (SWD) what allows the upload of firmware onto the MCU.

The goal was to develop a "pogo pin test bed" to be able to switch between multiple boards with minimal wear. But, due to the fact that two of the pads were too close, any 3d printed structure can assure a reliable print of the holes at the correct size and distance. In a future board, these two pads need to be placed further a part.

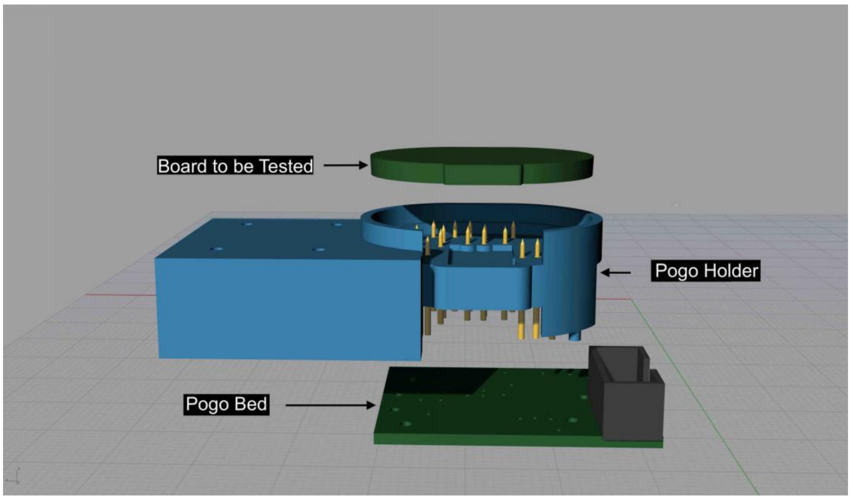

Figure 41 Pogo Pin bed test example

As for the firmware test goes, the MCU responded correctly to its firmware download that uses the Cortex-M4 core controlling the different GPIO. When trying to use the Cortex-M0 that controls BLE radio and contains the BLE stack, the test not go according what was done with the development board.

The best guess about that error is the configuration of the clock oscillators present, which needs to be accurate in order to maintain communication with other BLE devices.

The problem derives from the fact that the BLE code cannot be debugged because when the code execution is hijacked, the BLE stack of the other devices consider the connection failed and disconnects the communication.

These have been all the test done in the prototype board, being a good step towards a fully enclose insole design.

Gantt diagram & Budget

Figures 42 and 43, show the Gantt diagram made with the Gantt Project program, which allows visualizing the schedule of the project.

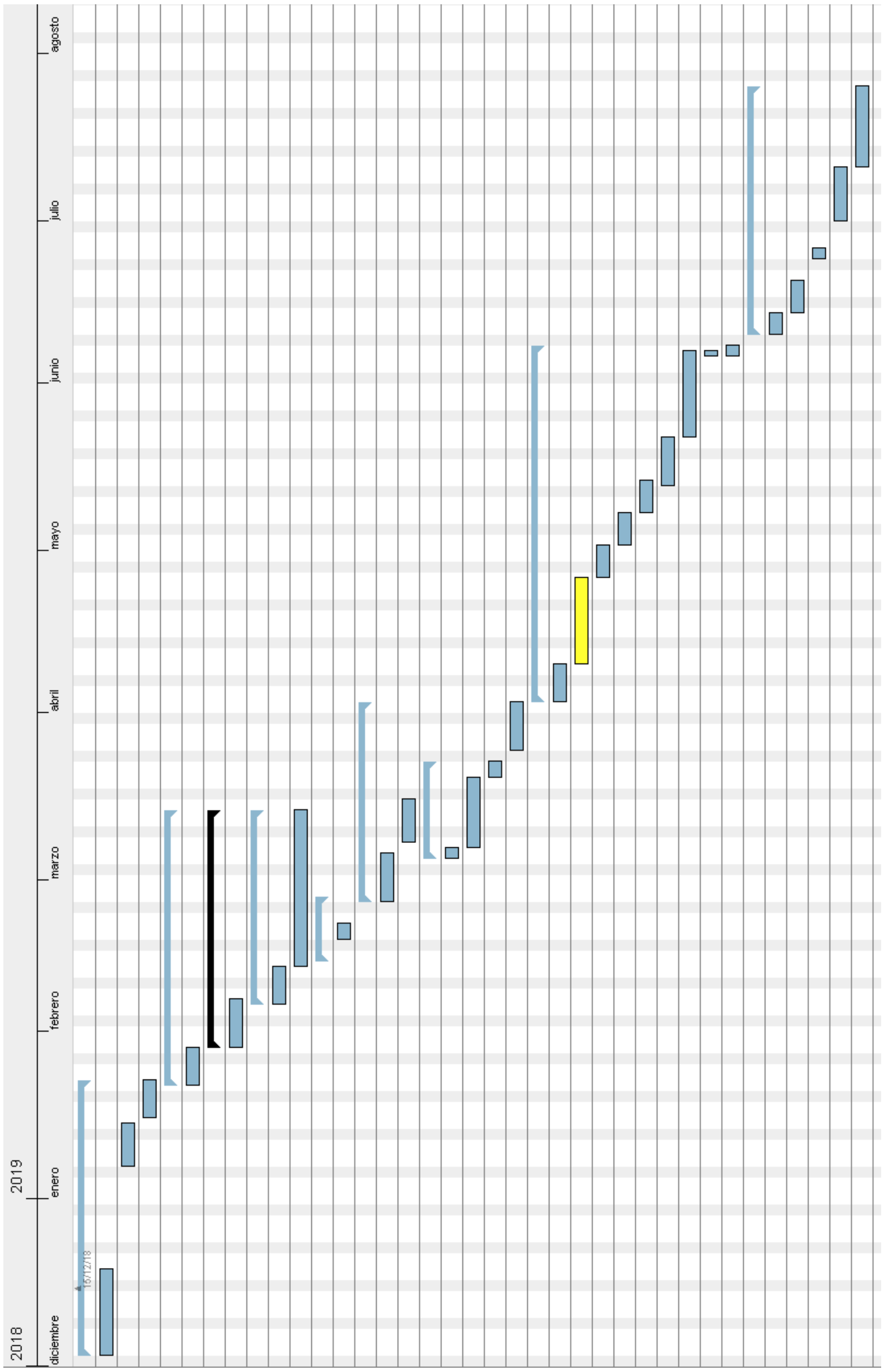

Figure 42 Gantt project timeline

Nombre	Fecha de inicio	Fecha de fin
Phase0 Definition and planification	3/12/18	22/01/19
Initial documentation lecture	3/12/18	18/12/18
Scheme elaboration	7/01/19	14/01/19
Definition work plan	16/01/19	22/01/19
Phase1 Architecture	22/01/19	13/03/19
Definition of the arquitecture	22/01/19	28/01/19
Component Selection	29/01/19	13/03/19
Logic Component Selection	29/01/19	6/02/19
LPWAN Selection	6/02/19	13/03/19
Study LPWAN technologies	6/02/19	12/02/19
Selection LPWAN selection	13/02/19	13/03/19
Power Board Selection	14/02/19	25/02/19
Qi Test	18/02/19	20/02/19
tarea_105	25/02/19	2/04/19
Toolchain Setup	25/02/19	5/03/19
Hello World	8/03/19	15/03/19
ADC Insole test	5/03/19	22/03/19
PCB Design	5/03/19	6/03/19
Manufacturing	7/03/19	19/03/19
Soldering and Testing	20/03/19	22/03/19
BLE test	25/03/19	2/04/19
Phase3 PCB design	3/04/19	7/06/19
Power Board Design	3/04/19	9/04/19
Vacaciones	10/04/19	25/04/19
MCU + IMU design	26/04/19	1/05/19
LoRa Desgin	2/05/19	7/05/19
Iteration 1	8/05/19	13/05/19
Interaction with Manufacturer	13/05/19	21/05/19
Manufacturing	22/05/19	6/06/19
Inspection	6/06/19	6/06/19
BoM generation	6/06/19	7/06/19
Phase4 Soldering and Testing	10/06/19	25/07/19
Ordering Components	10/06/19	13/06/19
Test Plan definition	14/06/19	19/06/19
Inspection Components	24/06/19	25/06/19
Power Board Soldering and Test	1/07/19	10/07/19
MCU Soldering and TEST	11/07/19	25/07/19

Figure 43 Detailed Gantt project timeline

Concerning the budget, the total cost is detailed in figure 44.

COST ESTIMATION FOR SERENE INSOLE (1 unit)			
Power Board			
Name	**Function**	**Cost (1u)**	**Cost (100u)**
STWLC33	IC ST for Qi	3.46€	2.55€
Wurth Antenna	Qi Antenna	7,70 ~12€	5,95~9,88€
TPS6303x	DC/DC converter	1,88€	1.35€
Coin Cell	Li-ion Battery	10~20€	5~14€
MLX92212LSE	Magnetic Switch	0,79€	0.552€
MCP73831/2	Battery Charger	0.490€	0.366€
	Various Passives	6,00€	
Logic Board			
Name	**Function**	**Cost (1u)**	**Cost (100u)**
STM32WB55xx	Main SoC (BLE)	7.20€	5.20€
SX1276	Semtech LoRa transceiver	6.82€	5.12€
FXP280	Flexible Antenna 868MHz	13,34€	10.52€
Atom FXP75	Flexible Antenna 2,4GHz	7,26€	5.12€
BNO055	9DOF IMU	9.21€	5.17€
Manufacturing			
Name	**Function**	**Cost**	
PCB	Rigi-flex PCB construction	80~200	

Figure 44 Budget breakdown

Looking at the table in Figure 44, we can see the breakdown of the budget. The two columns, one for the cost of 1 unit and one for the cost of 100 units is due to the fact that by purchasing large volumes of components, distributors make a significant discount on the price per unit and although there are components of which there is only one on the PCB, there are others, such as passive components, which are repeated.

With respect to the figure given in the PCB budget, the price variation depends on several factors. One of them is that of microvias although there are others such as the presence of rigid-flex, the finish and the manufacturing speed.

Results and Conclusions

The main objective of the project was to develop a first iteration of the electronics solution for a fully encapsulated insole, comfortable for the final user and resistant to the adverse environment in terms of weight and humidity. I achieved the generation a rigid-flex PCB able to fit in the insole with small enough dimensions.

There are aspects of this design that have not yet been tested and others that must be corrected. For those, I am proposing improvements such as using the same encapsulation in the development board as in the final PCB, as for the MCU BLE SoC. This was not possible for me and will make the programs generated in the prototyping phase fully compatible even losing the improvement in the unit price of the design.

Another aspect to bear in mind is that although the smaller the better, there comes a point that this maximum is not applicable. I am referring to the case of the passive (capacitors, resistance and inductances) used in the project.

When using too small packages (0201) many of the optimal values were not available while for 0402 packages they were. The improvement in terms of area using the former instead of the latter is negligible and considering that the first units are soldered by hand, a somewhat larger package allows on the one hand to have larger pads if repairs have to be made and on the other hand to be able to solder the components more easily.

Concerning the use of rigid-flex PCBs. Although for the final production will be in the design, currently it was an unnecessary expense from the point of view of prototyping. There is an additional cost factor at the time of PCB manufacture and a point of failure in terms of handling and soldering, where the heat generated in the soldering cycles could compromise the flexible material.

Another point to keep in mind is the connection between the pressure sensors and the electronics. Although the ACF tape works excellently, it is yet to be seen that it will be able to withstand the inclemency of the situations to which the electronics will be subjected during daily use.

Since low temperature soldering has been ruled out for having horrific results another solution that has not been tested in this project is the use of conductive epoxy glue to join the tracks. It should be tested if the silver ink tracks are compatible with that type of glue and if they hold for a reasonable lifespan.

Finally, although obvious, is the use of a Qi receiver for the transmission of power and so be able to charge the batteries of the device has to be changed. Although it was a component that had potential, it has turned out to be a continuous headache, because of its encapsulation, lack of availability and if samples had been obtained, the soldering process would have continued to be a problem.

If the aim is to reduce costs, the use of gold-plated contacts on the heel of the insole is a possibility as is already done in training products to prevent oxidation. If we wanted to continue with Qi, we should look for another receiver with similar characteristics.

I want to highlight the design ofthe Power board, where a high level of miniaturization is achieved with a power supply capable of provide the load of any peak consumption that the system could be in and the modularity of the battery charger.

References

[1] http://www.pharmatimes.com/news/nhs_to_fund_continuous_blood_glucose_monitoring_system_1260230

[2] http://www.coaguchek.com/coaguchek_patient/en/home/products/inrange.html

[3] https://www.ncbi.nlm.nih.gov/pmc/articles/PMC4114416/

[4] *Plantar pressure distribution and gait stability: Normal VS high heel* Sharvindsing Karia, S. Parasuraman, M. K. A. Ahamed Khan, I. Elamvazuthi, Niranjan Debnath, Syed Azhar Ali https://ieeexplore.ieee.org/document/7847822

[5] www.octopart.com

[6] https://www.st.com/en/development-tools/stm32cubemx.html

[7] Sensingtex web

[8] https://www.sciencedirect.com/topics/engineering/sensor-fusion

[9] Bandas de frecuencias no licenciadas. Nellith Plata. Enero 15, 2011

[10] https://www.link-labs.com/blog/what-is-lora

[11] https://www.wirelesspowerconsortium.com/blog/tipping-point-for-qi-adoption

[12] https://addi.ehu.es/bitstream/handle/10810/10666/PFC%20I.%20Carnero%20-%20Memoria.pdf

[13] http://www.minamoto.com/9-what-is-passivation-of-lithium-battery/

[14] AN3116Application noteSTM32™s ADC modesand their applications

https://www.st.com/content/ccc/resource/technical/document/application_note/c4/63/a9/f4/ae/f2/48/5d/CD00258017.pdf/files/CD00258017.pdf/jcr:content/translations/en.CD00258017.pdf

[15] https://www.st.com/resource/en/reference_manual/dm00318631.pdf

[16] https://www.researchgate.net/publication/259446328_Size-dependent_mechanical_behavior_of_nanoscale_polymer_particles_through_coarse-grained_molecular_dynamics_simulation

[17] https://resources.altium.com/pcb-design-blog/how-ultrafast-uv-lasers-improve-hdi-pcb-design-layouts

ANNEX

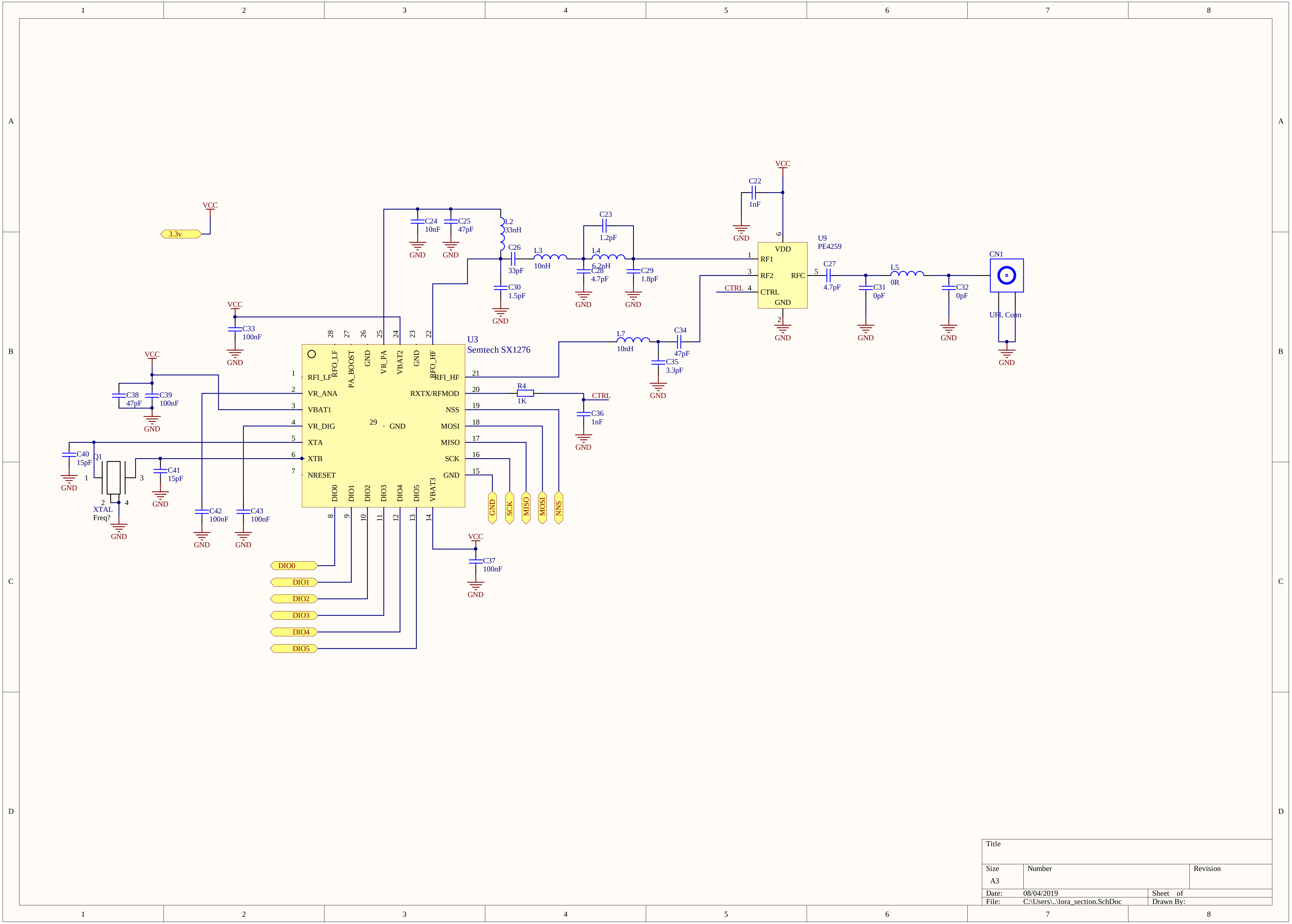

U3
Semtech SX1276
RFI_LF
VR_ANA
VBAT1
VR_DIG
XTA
XTB
NRESET
RFO_LF
PA_BOOST
GND
VR_PA
VBAT2
RFO_HF
RFI_HF
RXTX/RFMOD
NSS
MOSI
MISO
SCK
DIO0
DIO1
DIO2
DIO3
DIO4
DIO5
VBAT3
29
U9
PE4259
VDD
RF1
RF2
RFC
CTRL
CN1
UFL Conn
VCC
3.3v
C22 1nF
C23 1.2pF
C24 10nF
C25 47pF
C26 33pF
C27 4.7pF
C28 4.7pF
C29 1.8pF
C30 1.5pF
C31 0pF
C32 0pF
C33 100nF
C34 47pF
C35 3.3pF
C36 1nF
C37 100nF
C38 47pF
C39 100nF
C40 15pF
C41 15pF
C42 100nF
C43 100nF
L2 33nH
L3 10nH
L4 6.2nH
L5 0R
L7 10nH
R4 1K
Q1
XTAL
Freq?
Title
Size
A3
Number
Revision
Date: 08/04/2019
Sheet of
File: C:\Users\..\lora_section.SchDoc
Drawn By:

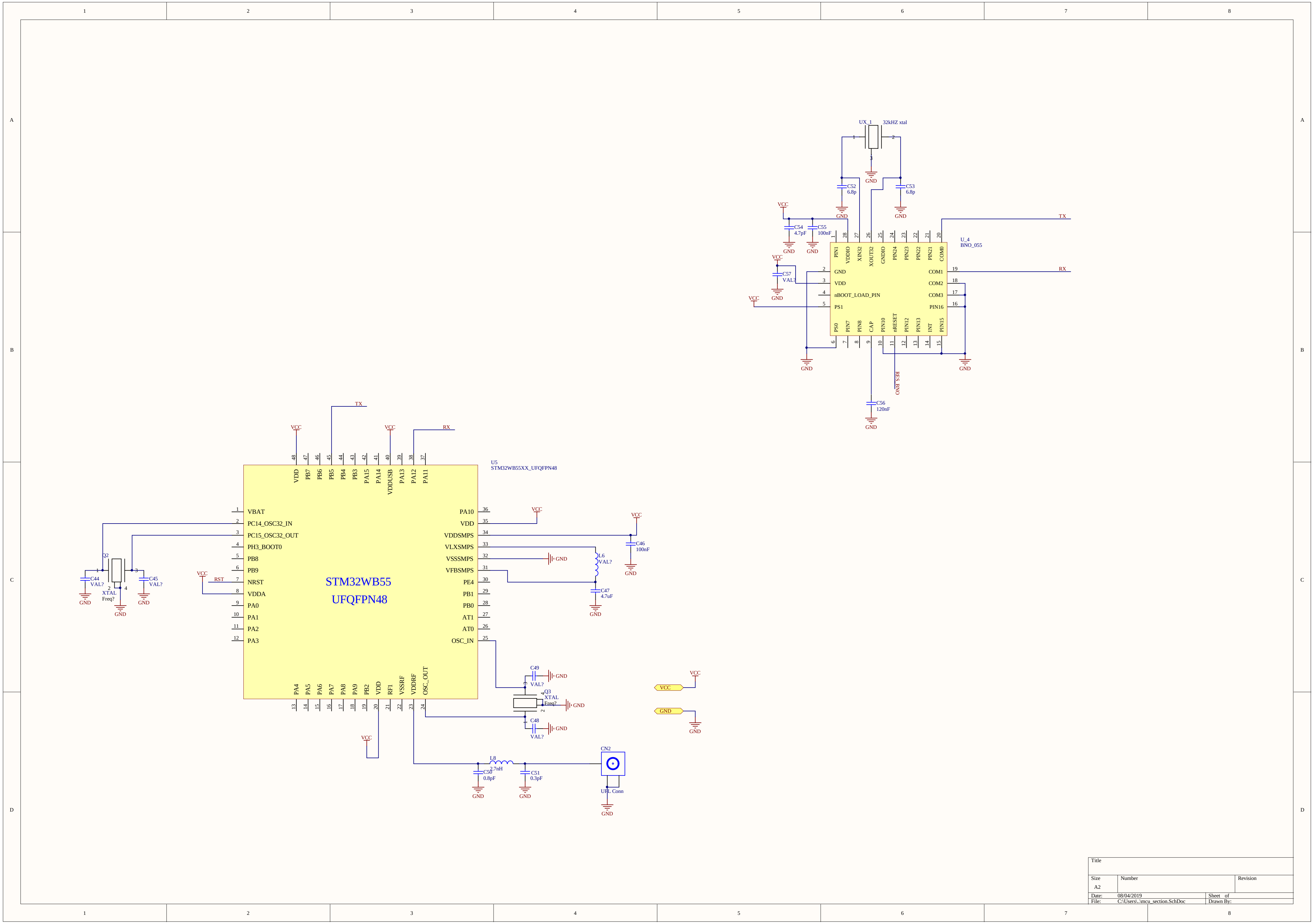

UX_1
32kHZ xtal
C52
6.8p
C53
6.8p
C54
4.7pF
C55
100nF
C57
VAL?
U_4
BNO_055
PIN1
VDDIO
XIN32
XOUT32
GNDIO
PIN24
PIN23
PIN22
PIN21
COM0
GND
VDD
nBOOT_LOAD_PIN
PS1
COM1
COM2
COM3
PIN16
PS0
PIN7
PIN8
CAP
PIN10
nRESET
PIN12
PIN13
INT
PIN15
TX
RX
RES_BNO
C56
120nF
U5
STM32WB55XX_UFQFPN48
STM32WB55
UFQFPN48
VDD
PB7
PB6
PB5
PB4
PB3
PA15
PA14
VDDUSB
PA13
PA12
PA11
VBAT
PC14_OSC32_IN
PC15_OSC32_OUT
PH3_BOOT0
PB8
PB9
NRST
VDDA
PA0
PA1
PA2
PA3
PA10
VDD
VDDSMPS
VLXSMPS
VSSSMPS
VFBSMPS
PE4
PB1
PB0
AT1
AT0
OSC_IN
PA4
PA5
PA6
PA7
PA8
PA9
PB2
VDD
RF1
VSSRF
VDDRF
OSC_OUT
Q2
XTAL
Freq?
C44
VAL?
C45
VAL?
RST
C46
100nF
L6
VAL?
C47
4.7uF
C49
VAL?
Q3
XTAL
Freq?
C48
VAL?
L8
2.7nH
C50
0.8pF
C51
0.3pF
CN2
UFL Conn
VCC
GND
Title
Size
A2
Number
Revision
Date:
08/04/2019
Sheet of
File:
C:\Users\..\mcu_section.SchDoc
Drawn By:

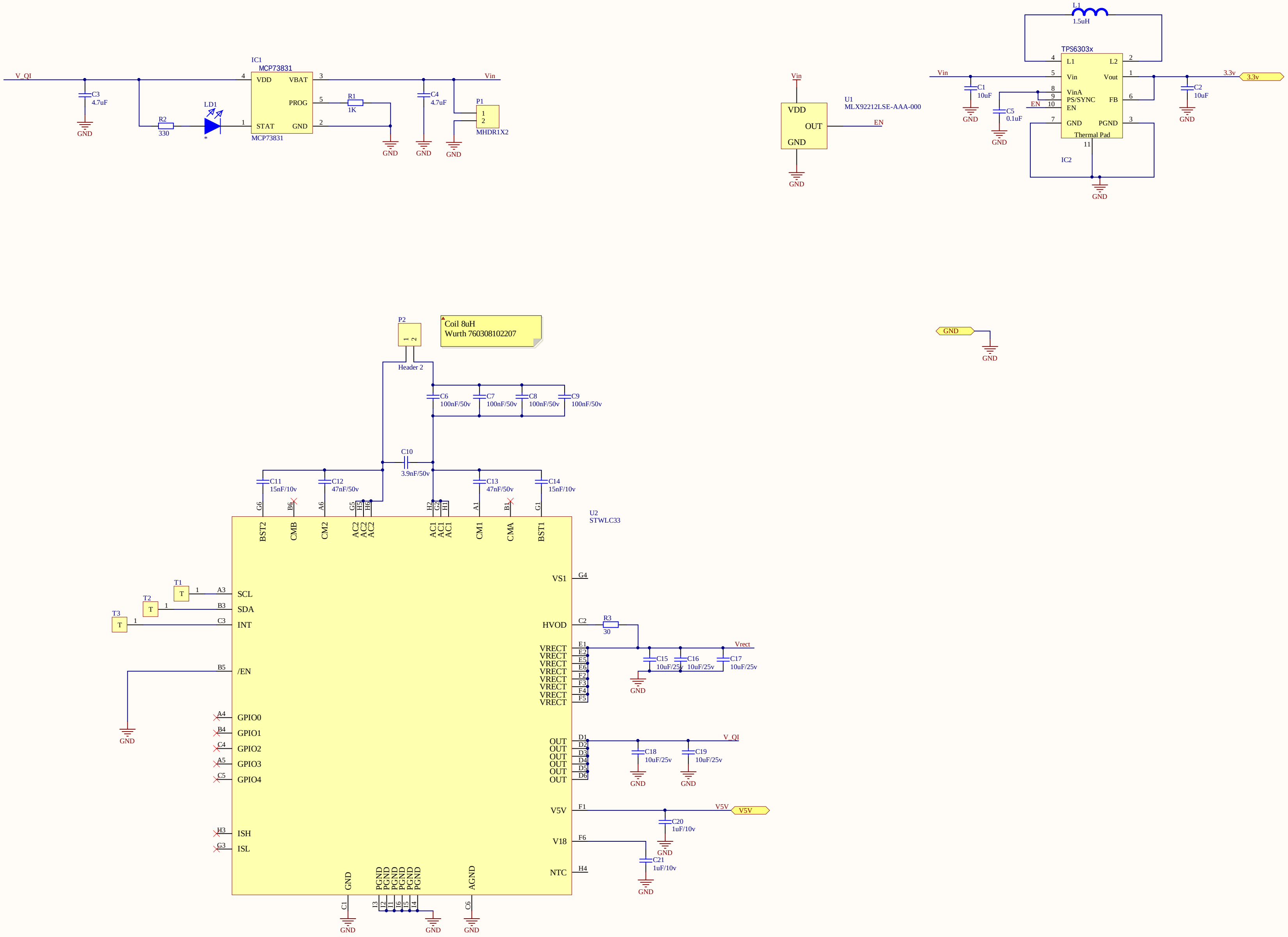

Title		
Size A2	Number	Revision
Date: 08/04/2019		Sheet of
File: C:\Users\..\power_section.SchDoc		Drawn By:

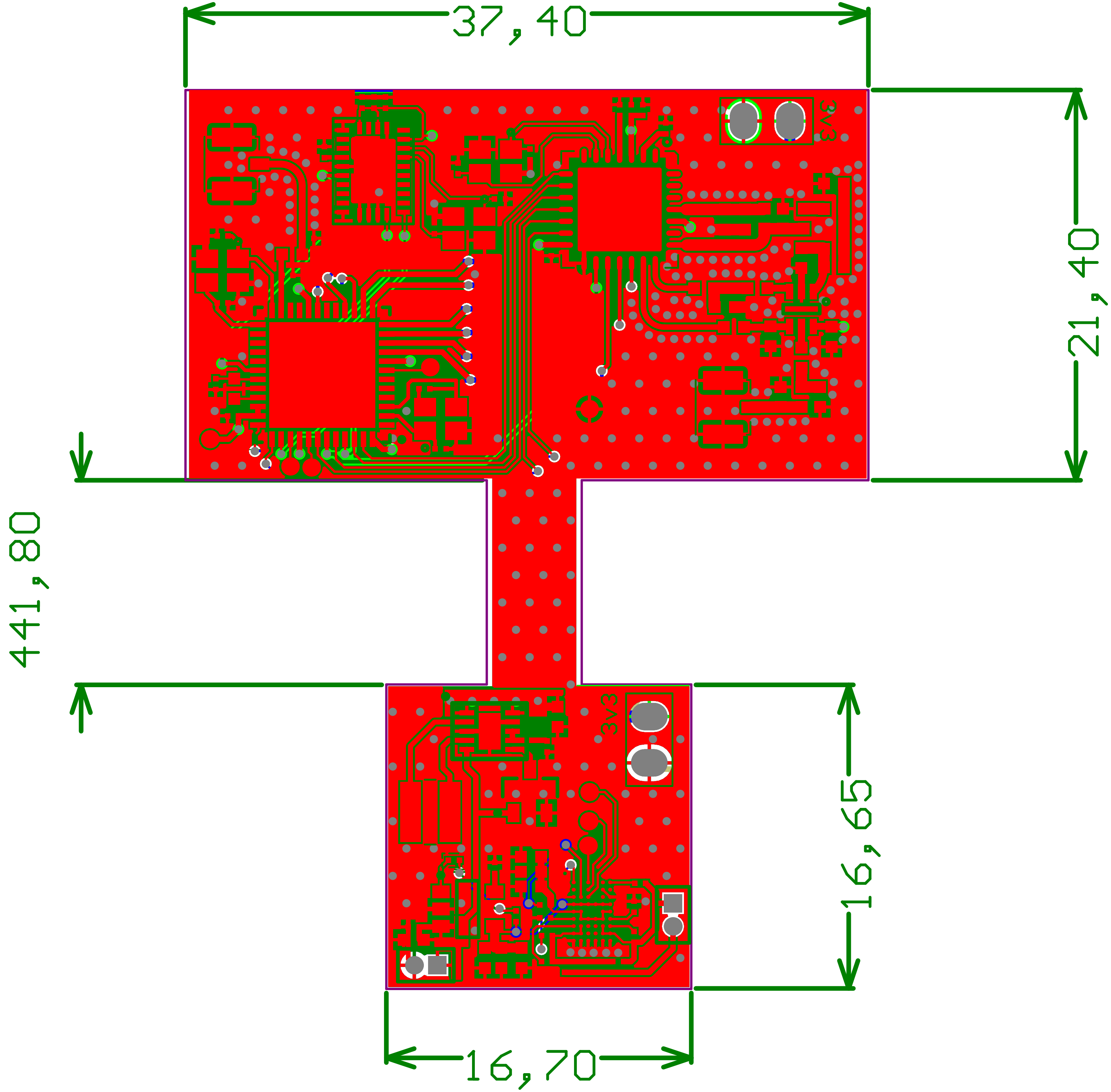
37,40
21,40
441,80
16,65
16,70
3V3
3V3

Comment	Description	Designator	Footprint	Quantity	Value	SKU	Price
Cap	Capacitor SMD	C1, C2	rlc_402_smd	2	10uF	2611904	0,177€@10u
Cap	Capacitor SMD	C3	rlc_402_smd	1	4.7uF	2688503	0,19€@10u
Cap	Capacitor SMD	C4	RLC_0201_SMD	1	4.7uF (Cambiado por 1uF)	2672085	0,139€@10u
Cap	Capacitor SMD	C5	RLC_0201_SMD	1	0.1uF	2528750	0,133€@10u
Cap	Capacitor SMD	C6, C7, C8, C9	RLC_0201_SMD	4	100nF/50v (cambiado de 50v	2611885	0,0238€@10u
Cap	Capacitor SMD	C10	RLC_0201_SMD	1	3.9nF/50v (cambiado de 50v	81-GRM33R61E392KA12D	0,014€@10u
Cap	Capacitor SMD	C11, C14	RLC_0201_SMD	2	15nF/10v	81-GCM033R71A152KA3D	0,04€@10u
Cap	Capacitor SMD	C12, C13	RLC_0201_SMD	2	47nF/50v (cambiado de 50v	81-GRM033R71E472KE4D	0,017€@10u
Cap	Capacitor SMD	C15, C16, C17, C18, C	rlc_402_smd	5	10uF/25v (cambiado de 25v	GRM155C80J106ME11D	0,14€@10u
Cap	Capacitor SMD	C20, C21	RLC_0201_SMD	2	1uF/10v	581-0201ZD105MAT2A	0,148€@10u
Cap	Capacitor SMD	C22, C36	rlc_402_smd	2	1nF	77-VJ0402Y102KXQCBC	0,192€@1u
Cap	Capacitor SMD	C23	rlc_402_smd	1	1.2pF	581-0101YA1R2BAT2A	0,281€@10u
Cap	Capacitor SMD	C24	rlc_402_smd	1	10nF	581-0402ZC103MAT2A	0,031€@10u
Cap	Capacitor SMD	C25, C34	rlc_402_smd	2	47pF	80-C0402C470J8G	0,178€@10u
Cap	Capacitor SMD	C26	rlc_402_smd	1	33pF	80-C0402C330K8G	0,173@10u
Cap	Capacitor SMD	C27, C28	rlc_402_smd	2	4.7pF	80-C0402C479K8G	0,169€@10u
Cap	Capacitor SMD	C29	rlc_402_smd	1	1.8pF	81-GJM0225C1C1R8CB1L	0,085€@10u
Cap	Capacitor SMD	C30	rlc_402_smd	1	1.5pF	81-GJM0225C1C1R5WB1L	0,196€@10u
Cap	Capacitor SMD	C31, C32	rlc_402_smd	2	0pF	No mounted	0
Cap	Capacitor SMD	C33	RLC_0201_SMD	1	100nF	81-GRM033C71A104KE4D	0,053€@10u
Cap	Capacitor SMD	C35	rlc_402_smd	1	3.3pF	81-GRM0225C1C3R3CA3L	0,045€@10u
Capacitor	Capacitor SMD	C38	RLC_0201_SMD	1	47pF	2576363	0,0184€@10u
Capacitor	Capacitor SMD	C39, C42, C43, C46, C	RLC_0201_SMD	5	100nF	81-GRM033C71A104KE4D	0,053€@10u
Capacitor	Capacitor SMD	C40, C41	RLC_0201_SMD	2	15pF	81-GCM0335C1E150JA6D	0,044€@10u
Capacitor	Capacitor SMD	C44, C45, C48, C49	RLC_0201_SMD	4	22pF	81-GJM0335C0J220JB1D	0,065€@10u
Capacitor	Capacitor SMD	C47	RLC_0201_SMD	1	4.7uF	81-GRM035R60J475ME5D	0,295€@10u
Capacitor	Capacitor SMD	C50	RLC_0201_SMD	1	0.8pF	81-GRM0335C1ER80BA1D	0,017€@10u
Capacitor	Capacitor SMD	C51	RLC_0201_SMD	1	0.3pF	81-GJM0335C1ER30BB01	0,071€@10u
Capacitor	Capacitor SMD	C52, C53	RLC_0201_SMD	2	6.8p	2906255	0,193€@10u
Capacitor	Capacitor SMD	C54, C57	RLC_0201_SMD	2	4.7pF	2434626	0,0183€@10u
Capacitor	Capacitor SMD	C56	RLC_0201_SMD	1	120nF (cambio a 150nF)	2526217	0,256€@10u
UFL Conn	UFL Hirose U.FL-R-SMT-1(10)	CN1, CN2	UFL Conn	2		1688077	0,816€@10u
PIN_1x2	Tira de pines 2 contactos	CN4, CN5	PIN_1x2	2	NO mounted	No Mounted	
MCP73831	Miniature single-cell, Li-ion/Li-Po charge	IC1	MCP73831	1		1332158	0,484€@10u
TSP6303x	TSP6303x Buck/boost converter single ir	IC2	TPS6303x	1		1689433	1,82€@1u
LPS3015	LPS3015 Shielded SMT Power Inductor	L1	LPS-3015	1	1.5uH	2408018	1,55€@1u
Inductor	Inductor	L2	rlc_402_smd	1	33nH	810-MLG0402Q33NJT000	0,214€@10u
Inductor	Inductor	L3, L7	rlc_402_smd	2	10nH	810-MHQ0402PSA10NHT	0,074€@10u
Inductor	Inductor	L4	rlc_402_smd	1	6.2nH	810-MLG1005S6N2HT000	0,038€@10u
Inductor	Inductor	L5	rlc_402_smd	1	0R	755-SFR01MZPJ000	0,056€@10u
Inductor	Inductor	L6	rlc_402_smd	1	10uH	81-LQW15DN100M00D	1,81€@10u
Inductor	Inductor	L8	rlc_402_smd	1	2.7nH	810-MLG1005S2N7CT000	0,038€@10u

LED	LED	LD1	0201 - LED	1	LED	696-SMLLX0201UPGCTR	0,242@10u
MHDR1X2	Header, 2-Pin	P1, P2	MHDR1X2	2	Paso 1,27mm	No mounted	No mounted
XTAL	Crystal with GND pins	Q1, Q2, UX_1	ND_2520	3	32.768 KHz	1674695	1,41€@10u
XTAL	Crystal with GND pins	Q3	ND_2520	1	16MHz	2469941	0,722€@10u
Resistor	Resistor SMD - IEC symbol version	R1	RLC_0201_SMD	1	1K	603-AC0201FR-071KL	0,048€@10u
Resistor	Resistor SMD - IEC symbol version	R2	RLC_0201_SMD	1	330	652-CR0201-JW-331GLF	0,083€@10u
Resistor	Resistor SMD - IEC symbol version	R3	RLC_0201_SMD	1	30	71-CRCW020130R0FNED	0,063€@10u
Resistor	Resistor SMD - IEC symbol version	R4	rlc_402_smd	1	1K	755-SFR01MZPJ102	0,056€@10u
Resistor	Resistor SMD - IEC symbol version	R5, R6, R7, R8, R9, R1(	rlc_402_smd	6	10k	755-SFR01MZPF1002	0,069€@10u
test point	Punto de testeo 1mm	T1, T2, T3, T4, T5, T6, '	test_point	8	######################	########################	#####################
MLX92212LSE-AAA-000	3-Wire Hall Effect Latch	U1	SOT23	1	######################	482-92212LSEAAA000RE	0,777€@1u
STWLC33_!!!!PAD REMOV	Multi-mode Qi/AirFuel inductive wireles	U2	STWLC33 - PADS DELETED!	1	######################		
Semtech SX1276	Semtech SX1276	U3	vqfn28_6x6mm	1		947-SX1276IMLTRT	7,04€@1u
STM32WB55XX_UFQFPN4	SoC BLE STM32	U4	STM32WB55xx UFQFPN48 p	1		#################	#####################
PE4259	RF Switch	U9	Peregrine PE4259	1		#################	#####################
BNO_055	IMU	U_4	BNO_055	1		262-BNO055	9,25€@1u (8.32€@10u)

Task	Method	Result	Comment	Action	Files
Soldering of the Buck/boost (with passive) and the battery charger.	Apply voltage in the range (2.7, 4.6v) at the battery connector. 3.3v regulated are expected	FAIL	Hall switch, wrong footprint, solder cable from enable to C5 to create a enable state in the regulator	Change at the PCB design	No
Soldering of the MCU (with passives).	Visual inspection to check for faulty connections/ tombstone (0201)	OK	None	None	No
Program the MCU (soldering cables to SWD pads)	Download FW elementary code (hello world)	OK	Complex programming with probes	Create a PCB with pogo pins to provide 3.3v and SWD	filename, app
Load software into MCU to test BLE coms	Add 2.4GHz Antenna, download Stdemo code, check with APP		pairing, STM32_2_APP (fixed sensor values), APP_2_STM32 (toggle output)		
Soldering IMU sensor, and passives	Visual inspection to check for faulty connections/ tombstone (0201)				
Test the MCU SW for the IMU	Read IME values changing the board orientation (gravity vector, motion angles, magnetic pole)		Acceleration, gyro, magnetic sensors		
Test the MCU SW for the IMU cortexM0	Read trajectory (or quaternions or Euler angles) to veryfy the M0 compuation		motion parameters		
Test the MCU SW for the IMU ranges	Configuraion capabilities & range scale		configuration capabilities		
Soldering LoRa transceiver, and passives for the line transmission	Visual inspection to check for faulty connections/ tombstone (0201)				
Test the software of the LoRa sending frames to our getway to test the correct functionality	Add 868MHz Antenna, download demo code, check with Lora server				
Test the insole pressure sensors	Add insole sanple data, sent by bluetooth, check with the apps (and tailored weights)				
Soldering Qi RX and passives for wireless charging	Visual inspection to check for faulty connections/ tombstone (0201)				
Test the Qi wireless charging	Check the St component, antenna. Use the ST Qi kit				